NASA
Reference
Publication
1323

November 1993

Nimbus–7 Total Ozone Mapping Spectrometer (TOMS) Data Products User's Guide

Richard D. McPeters, Arlin J. Krueger, P.K. Bhartia,
Jay R. Herman, Arnold Oaks, Ziuddin Ahmad,
Richard P. Cebula, Barry M. Schlesinger, Tom Swissler,
Steven L. Taylor, Omar Torres, and Charles G. Wellemeyer

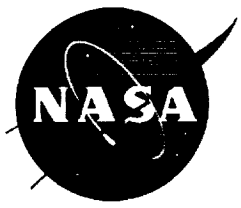

NASA Reference Publication 1323

November 1993

Nimbus–7 Total Ozone Mapping Spectrometer (TOMS) Data Products User's Guide

Richard D. McPeters, Arlin J. Krueger, P.K. Bhartia, Jay R. Herman, Arnold Oaks
Goddard Space Flight Center
Greenbelt, Maryland

Ziuddin Ahmad, Richard P. Cebula, Barry M. Schlesinger, Tom Swissler, Steven L. Taylor, Omar Torres, and Charles G. Wellemeyer
Hughes STX Corporation
Lanham, Maryland

National Aeronautics and Space Administration

Scientific and Technical Information Branch

ACKNOWLEDGMENTS

The HDTOMS and GRIDTOMS tapes described in this User's Guide were prepared by the Ozone Processing Team (OPT) of NASA/Goddard Space Flight Center. Please acknowledge the Ozone Processing Team as the source of these data whenever reporting on results obtained using the HDTOMS and GRIDTOMS tapes. A complete list of OPT members is provided in Section 2.6.

We offer a special acknowledgement to our colleague Arnie Oakes who passed away before our completion of this work. His contributions as Nimbus Project Manager were innumerable. His positive attitude and head-on approach to problems combined with his frank and open personality made him a pleasure to work with. We all have benefitted from his presence, and we continue to benefit from his memory.

TABLE OF CONTENTS

TABLE OF CONTENTS (Continued)

LIST OF FIGURES

LIST OF TABLES

SECTION 1

INTRODUCTION

This document is a guide to the data products obtained from the measurements by the Total Ozone Mapping Spectrometer (TOMS) experiment aboard the Nimbus–7 satellite. It discusses the calibration of the instrument, the algorithm used to derive ozone values from the measurements, the uncertainties of the data on the tapes, and the tape structure. The data on the tapes begin October 31, 1978 and end May 6, 1993. These data are archived at the National Space Science Data Center (NSSDC).

When the previously archived Version 5 TOMS data were found to have a long-term calibration drift (Flieg *et al.*, 1986a, 1986b, 1988, 1989; Watson and Ozone Trends Panel, 1988, 1990; Hudson *et al.*, 1989; and Herman *et al.*, 1990), an improved internal calibration technique, the Pair Justification Method (PJM) was developed (Herman *et al.*, 1991). The currently archived Version 6 TOMS data have a long-term calibration accuracy of $\pm$ 1.5 % in total ozone. The new TOMS products described in this document supersede the previously archived products, and this document supersedes previous documents describing those products.

Nimbus-7 was launched on 24 October 1978; measurements began about a week later. For the purpose of obtaining daily high-resolution global maps of atmospheric ozone, TOMS measures the solar irradiance and the radiance backscattered by the Earth's atmosphere in six selected wavelength bands in the ultraviolet. The algorithm described in this document is used to retrieve total column ozone (also referred to as total ozone) from these radiances and irradiances. TOMS maps total ozone by scanning in 3° steps to 51° on each side of the subsatellite point, in a direction perpendicular to the orbital plane. Consecutive cross-scans overlap, creating a contiguous mapping of ozone.

Section 2 relates this document and the data products it describes to previous documents and data products, listing the earlier versions and the changes between the current data products and the previous products. There are changes in both the derivation of the ozone values and in the format of the tapes. The tape formats for Version 6, however, are identical to those of Version 5. The changes that began in November 1984 are also described in Section 2. Section 3 provides a general overview of the TOMS instrument, the algorithm, the uncertainties in the results, and of other basic information required for best use of the tapes. It is designed for the user who wants a basic understanding of the products but does not wish to go into details. Such a user may wish to skip Sections 4 through 8. Section 4 presents an outline of those aspects of the theory of scattering of solar radiation by the Earth's atmosphere applicable to the retrieval of total ozone from backscattered radiances. In Section 5, the instrument, its calibration, and the characterization of its changes with time are discussed. The algorithm for retrieval of total ozone is described in Section 6. Section 7 describes the overall uncertainties in the ozone data and how they are estimated, while Section 8 discusses particular problems that affect limited time intervals and geographical areas. Detailed descriptions of the tape formats appear in Section 9. Appendix A provides a detailed discussion of the data quality flags. Appendix B provides sample FORTRAN programs that can be used to read the tapes. Appendices C and D tabulate information used in the algorithm for ozone retrieval, and Appendix E provides information on data availability.

SECTION 2

HISTORICAL BACKGROUND

2.1 Processing History

The 14.5 years of TOMS data (31 October 1978 - 6 May 1993) were processed using the procedures described in this document, and were archived at the National Space Science Data Center (NSSDC) during the period between September 1990 and November 1993. The values were generated using Version 6.0 of the processing software. Versions 1-3 were developmental versions, and Version 4 was the first data released to the data archive. In 1985, Version 5 replaced Version 4 in order to use the newly approved Bass and Paur ozone absorption coefficients in place of the Inn and Tanaka coefficients used in Version 4. After the Ozone Trend Panel confirmed that error in the correction for the diffuser plate degradation was causing significant drift in the derived total ozone, a new technique was implemented to derive the relative calibration based on inter-pair consistencies (PJM). The entire TOMS data set was reprocessed using this stabilized long-term calibration and released as Version 6 in November of 1990. Version 6 data should be used for any future studies based upon TOMS measurements. The version of data on a tape can be identified from the tape generation data in the Standard Header File. Data on a tape can be identified as Version 6 if the generation date is on or after day 1 of 1990 or if it is explicitly identified as Version 6 in the Standard Header File. The format of Standard Header Files is described in Section 9.1 for HDTOMS tapes and in Section 9.2 for GRIDTOMS. The differences between Versions 5 and 6 are described in Section 2.3. The differences between Versions 4 and 5 are briefly described in Section 2.4.

In November 1984, some changes were made in the processing procedure in order to reduce the time between the actual measurements and the release of these data. The diffuser exposure time used in the calculation of the albedo calibration function is now a projection based upon the schedule for diffuser deployment, rather than, as in earlier years, the actual elapsed time. Finally, changes in the instrument performance that started in April 1984 have introduced a small, intermittent error. The size of this error and its frequency are discussed in Section 8.2.

2.2 Documentation History

The basic tapes from which other tape products are ultimately derived are the Raw Unit Tapes - TOMS (RUT-T). These tapes contain uncalibrated irradiance and radiance data, housekeeping data, calibration information, instrument field-of-view (FOV) location, and solar ephemeris information from TOMS. These tapes also contain information on terrain pressure and snow-ice thickness as well as some limited information on clouds. These tapes are discussed in a user's guide (Fleig *et al.*, 1983), which describes the experiment, instrument calibration, operating schedules and data coverage, data quality assessment, and tape formats applicable to the first two years. The contents of this user's guide are by and large still valid. The section on in-orbit instrument performance has been superseded.

In June 1982, a user's guide to the first year of TOMS data (Fleig *et al.*, 1982) was produced, to accompany the release of those data. In addition to describing the format of the released

OZONE-T tape, that user's guide described the algorithm used to retrieve ozone and provided a brief outline of its theoretical foundations. The description of the algorithm in the present guide is based upon the discussion in that document. The HDTOMS tape discussed here corresponds to the earlier OZONE-T.

In 1983, a new product was developed: GRIDTOMS, a tape containing daily averages of ozone over cells in a latitude-longitude grid. A tape specifications document was issued to accompany the tapes.

As the baseline of time available for deriving the instrument calibration increased, additional improvements in the characterization of the changes with time became possible. By the time four years of data were to be archived, a revised characterization function had been developed. In addition, El Chichón had erupted, and provision needed to be made for identifying ozone retrievals that might be contaminated by SO_2 ejected by the eruption. There had also been some changes in the tape format. These issues were addressed in a third- and fourth-year addendum to the first-year user's guide (NASA, 1984). This document included, in addition, a catalog of high-density TOMS (HDTOMS) tapes for the third and fourth years of measurements.

After eight years of data were available, it became apparent that further refinement of the long-term calibration of the TOMS was required. An improved long-term calibration, described in Section 5.4, and minor modifications of the algorithm, described in Section 2.3, were incorporated into Version 6 TOMS processing.

The present user's guide is intended to supersede all previous documents on the ozone tape products (Fleig *et al.*, 1982; NASA, 1984), but not the entire RUT User's Guide (Fleig *et al.*, 1983). The tape format in the GRIDTOMS specifications has been incorporated into Section 9 and the supplemental discussion, into other parts of this document.

2.3 Changes Between Version 5 and Version 6

The central motivation for the Version 6 reprocessing was to apply a long-term calibration correction to the Version 5 data set. This correction is described in Section 5.4. Some improvements to the algorithm were also incorporated including updated Antarctic ozone climatology, corrected errors in attitude determination, redefinition of B-pair ozone wavelengths, and recomputation of pair calibration adjustment factors.

Antarctic Climatology

The TOMS total ozone retrieval algorithm is a table look-up and interpolation process. The precomputed table contains backscattered radiance as a function of total ozone, optical slant path length, surface pressure, surface reflectivity, and latitude. Table values are computed based on a set of assumed climatological ozone and temperature profiles. Due to the extreme conditions that have developed over the Antarctic Continent during the latter part of the TOMS lifetime, it has been necessary to expand this set of standard profiles to improve the TOMS retrieval during "ozone hole" conditions. The Version 5 ozone profiles misrepresent the shape of the typical ozone hole profile and over-predict the "depth" of the ozone hole, in this case by 4 - 7 D.U. at 76 degrees solar zenith angle, and 4 - 10 D.U. at 86 degrees solar zenith angle. The Version 5 temperature profiles are too warm and also have the effect of over-predicting the "depth" of the

ozone hole by 3 - 3.5 D.U. at 76 degrees solar zenith angle, and 0.5 - 1.5 D.U. at 86 degrees solar zenith angle (this error behaves like a calibration error and becomes smaller at higher path length). The drift of the Version 5 calibration also tends to over-predict the depth of the ozone hole by about 6 D.U. The Version 6 look-up tables have been extended to include typical "ozone hole" ozone and temperature profiles, so that the errors mentioned above should be minimized in the new data set.

Attitude Determination Corrections

Some small errors have been identified in the computation of the Nimbus-7 spacecraft attitude. These errors affect the determination of the viewing geometry associated with each measurement, but they are so small that significant error in total ozone determination occurs only at the extreme off-nadir scan positions, where small errors in spacecraft roll angle affect the path length determined for the backscattered radiation. The identified errors are of the order of 0.1 degree in roll and correlate both empirically and theoretically with the cross-track bias (of the order of 2 D.U.) observed in the Version 5 TOMS total ozone. The average equatorial cross-track bias has been used along with computed sensitivities to errors in spacecraft roll-angle determination to estimate a roll-angle correction to the original attitude determination. This indirect method was used in preference to a recomputation of attitude and viewing geometry, which would involve considerable resources. Some evidence of a small latitude dependence in this error was developed, but not taken into account by this approach. The return path length is much less critical at high solar zenith angles, so the associated error in the Version 6 product should be quite small.

Redefinition of TOMS B-pair Wavelengths and Recomputation of Pair Adjustment Factors

Starting in early 1984, the TOMS instrument began to develop an intermittent loss of synchronization between its wavelength selection/chopper wheel and the photon counting electronics [Fleig *et al.*, 1986a]. The synchronization error is small and appears as an increased level of noise in the total ozone retrieved from TOMS. In the summer of 1990, the incidence of the synchronization error increased to over 90 percent before dropping to near zero again in March of 1991. As described in further detail in Section 8.2, this noise is reduced by 40 percent if the B′-pair (317.5 nm - 339.8 nm) is used instead of the B′-pair (317.5 nm - 331.2 nm) used in the Version 5 processing. Because of its wider wavelength separation, the B′-pair is somewhat more susceptible to wavelength dependence of scene reflectivity, but in the presence of nonsync, the B′-pair is clearly superior. In conjunction with the use of the B′-pair, the pair adjustment factors were recomputed for the Version 6 processing as well.

As described below in Section 6, the best ozone retrieved by the TOMS algorithm is the weighted average of total ozone determined by the A-pair, B-pair, and C-pair:

$$\text{Best} = (W_A f_A \Omega_A + W_B f_B \Omega_B + W_C f_C \Omega_C) / (W_A + W_B + W_C)$$

The adjustment factors f_A, f_B, and f_C have been selected to remove biases between the ozone values derived from the different pairs. These biases are the result of small inconsistencies in the

original instrument calculation. The factors are derived by comparing ozone from two pairs in a region where both provide information. Due to the use of the B′-pair in Version 6, these factors have been rederived and an improved C-pair factor (f_c) has also been computed. The factors for Version 5 were 1.0, 1.01, and 1.02 for the A, B, and C-pairs, respectively. The Version 6 adjustment factors are 1.0, 1.022, 1.034. The weights accorded the different pairs are a function of the wavelength separation of the pair and the pair sensitivity to total ozone at a given set of measurement conditions. Because of its wider wavelength separation, the B′-pair used in the Version 6 processing is given less weight than the B-pair used in Version 5. Over most of the globe, the A-pair and B-pair have weights of approximately 0.65 and 0.35, respectively, in Version 5 and 0.75 and 0.25 in Version 6.

2.4 Changes Between Version 4 and Version 5

There are a number of differences between the processing that generated the previously archived Version 5 data set and the previously archived Version 4 data set. These changes were in the analysis of the change with time of the instrument sensitivity, in the values of physical constants used for the retrievals, in the retrieval algorithm, and in the tape formats.

New values for the ozone absorption coefficients were incorporated into the revised algorithm. These coefficients are based on more recent measurements of ozone cross-sections (Paur and Bass, 1985) and were recommended for use in ozone measurement by the International Ozone Commission in its August 1984 meeting at Halkidiki, Greece. The change in ozone absorption coefficients was the most significant improvement between Versions 4 and 5. Small changes in the Rayleigh scattering coefficients were also made to incorporate some recently published data (Bates, 1984). Table 6.1 contains the ozone absorption and Rayleigh scattering coefficients at the TOMS wavelengths.

In addition, the total ozone and profile data quality flags were redefined. These flags now provide considerably more information about the data quality and allow the user to select slightly contaminated or less reliable data if necessary. However, users must now pay careful attention to the meaning of these flags in order to avoid inadvertently selecting bad data. Section 3.3 provides definitions for the flags and recommendations as to which should be accepted. A more detailed discussion of the reasons for flagging or not flagging data appears in Section 6.5.

2.5 Experiment Team

The combined SBUV/TOMS instrument has been supported by the Nimbus Experiment Team (NET). The original members of NET were D. F. Heath, Chairman; A. J. Krueger, C. L. Mateer, A. J. Miller, D. Cunnold, A. E. Green, A. Belmont, and W. L. Imhof. In addition, A. J. Fleig, R. D. McPeters, A. Kaveeshwar, K. F. Klenk, P. K. Bhartia, and H. Park were nominated by NET to be Associate Members. The TOMS instrument was built by Beckman Instruments, Inc., of Anaheim, California.

2.6 Ozone Processing Team (OPT)

The TOMS algorithm development, evaluation of instrument performance, ground-truth validation, and data production were carried out by the Ozone Processing Team (OPT) at NASA/GSFC. The OPT is managed by the Nimbus Project Scientist, R. D. McPeters. The current OPT members include:

Z. Ahmad, E. Beach, P. Bhartia, W. Byerly, R. Cebula, S. Chandra, S. Cox, M. Deland, L. Flynn, J. Gleason, X. Gu, J. Herman, E. Hilsenrath, R. Hudson, G. Jaross, A. Krueger, G. Labow, D. Larko, J. Leitch, J. Lienesch, T. Miles, J. Miller, R. Nagatoni, P. Newman, H. Park, B. Raines, C. Seftor, T. Swissler, J. Stokes, R. Stolarski, S. Taylor, O. Torres, and C. Wellemeyer.

The original OPT was managed by A. J. Fleig, the previous Nimbus Project Scientist. Previous members of the OPT include:

L. Bowlin, G. Chalef, M. Forman, J. Fredrick, J. Gatlin, D. Gordon, B. Guenther, M. Hinman, J. Hurley, A. Kaveeshwar, K. Klenk, K. Lee, B. Lowry, B. Monosmith, N. Oslik, V. Pavanasaisam, S. Ray, S. Reed, J. Schneider, D. Silberstein, P. Smith, S. Truong, and C. Wong.

SECTION 3

OVERVIEW

3.1 Instrument

The Total Ozone Mapping Spectrometer (TOMS) experiment on board the Nimbus-7 satellite provides daily global coverage of the Earth's total ozone by measuring the ultraviolet albedo–the ratio of backscattered Earth radiance to incoming solar irradiance–in the six 1-nm bands listed in Table 5.1. The experiment uses a single monochromator and scanning mirror to sample the backscattered solar ultraviolet radiation at 35 sample points at 3-degree intervals along a line perpendicular to the orbital plane. The measurements used for ozone retrieval are made during the sunlit portions of the orbit as the spacecraft moves from south to north. In normal operation, the scanner measures 35 scenes, one for each scanner view angle stepping from right to left. It then quickly returns to the first position, not making measurements on the retrace. Eight seconds after the start of the previous scan, another begins.

To measure the incident solar irradiance, a ground aluminum diffuser plate, common to both the SBUV and TOMS systems, is deployed to reflect sunlight into the instrument. The only difference between the system used to measure Earth radiance and that used to measure solar irradiance is the deployment of the diffuser plate when solar irradiance is being measured; the other optical components are identical. Therefore, the only change in the instrument that can cause a change of the albedo with time is a change in the reflectivity of the diffuser plate. Changes in any other aspect of the optical system will affect both radiance and irradiance in the same way; their effects will cancel when the albedo is calculated from the ratio of radiance to irradiance. Because the same diffuser plate is used for both SBUV and TOMS, and because daily continuous scan measurements were made using SBUV while only weekly solar measurements at the six discrete wavelengths were available for TOMS, a diffuser degradation characterization derived using SBUV measurements has been used in the TOMS ozone retrievals.

A more detailed description of the instrument and its calibration appears in Section 5.

For the first 7½ months of operation, TOMS followed a regular ON/OFF schedule for spacecraft power management, operating on 10 of each 12 days. At times, the instrument was operated on scheduled OFF days also, thus resulting in an actual duty cycle greater than 83 percent. A relay malfunction prevented any measurements from being made during the 6-day period June 14-19, 1979. Since June 22, 1979, TOMS has operated full time.

3.2 Algorithm

The retrieval of total ozone is based on a table look-up and interpolation process. A table is constructed that gives backscattered radiance as a function of total ozone, optical slant path length, surface pressure, surface reflectivity, and latitude. Given the computed radiances for the latitude, surface pressure, reflectivity, and slant path for a particular radiance measurement, the total ozone value for the scan can be derived by interpolation in the table.

Section 6 describes the algorithm in greater detail.

3.3 Data Uncertainties

The ozone values derived from the TOMS measurements have three types of uncertainties: uncertainties in the basic measurements, uncertainties in the physical quantities used to retrieve ozone values from the measurements, and uncertainties in the mathematical procedure used to retrieve ozone values from the measurements. Each of these sources of uncertainty can be manifested in one or more of three ways: random error, an absolute error that is independent of time, and a time-dependent error, or drift. For TOMS total ozone, the absolute error is ± 3 percent, the random error is ± 2 percent (1σ) and the drift for 14 years is ± 1.5 percent though somewhat higher at high latitudes. More detailed descriptions of the different sources of uncertainty and the extent to which each contributes to the overall uncertainty appear in Sections 5, 7, and 8. Starting in 1984, an instrument problem developed, which led to a small increase in the random error of approximately 1 D.U. Further discussion of this problem is provided in Section 8.2.

The difference between the TOMS and Dobson total ozone measurements at the time of the Nimbus-7 launch was approximately 1 percent, with TOMS reporting higher ozone values. However, TOMS total ozone values have been derived using the ozone absorption cross-sections measured at the U.S. National Bureau of Standards (Paur and Bass, 1985). The Dobson network has now (1992) also adopted the more accurate new absorption cross-sections. With the Dobson measurements adjusted for the new ozone cross-sections, the TOMS-Dobson bias at launch increases to approximately 3-4 percent. It is likely that the TOMS values are too high (possibly because of inadequate bandpass characterization) since TOMS ozone values are also 3 percent higher than the SBUV instrument on the same satellite.

Comparisons with the Dobson network in 1988 (Fleig, Bhartia, and Silberstein, 1986; Fleig *et al.*, 1988b) showed that the TOMS-derived total ozone then archived (Version 5.0) drifted significantly against the ground-based observations. The 1988 Ozone Trends Panel (Watson and the Ozone Trends Panel, 1988) concluded that the technique used for maintaining the long-term calibration of the instrument (Cebula, Park and Heath, 1988) had large uncertainties, which made Version 5.0 SBUV data unsuitable for studies of long-term trends in atmospheric ozone.

Subsequent to the panel report, a new technique has been developed to improve the calibration of the instrument. The Pair Justification Method (PJM) has been used to correct the TOMS calibration drifts (Herman *et al.*, 1991). The PJM compares total ozone derived from two wavelength pairs that respond similarly to true ozone changes, but have different sensitivities to instrument calibration errors. By monitoring the difference in ozone derived from the two pairs as a function of time, it has been possible to estimate the long-term drifts in the four longest wavelengths of the SBUV instrument. Total ozone data produced from the TOMS instrument, corrected using the same technique, show no significant drift against the collocated measurements from the ground-based Dobson instruments (McPeters and Komhyr, 1991; Gleason *et al.*, 1993), even after 14 years of continuous operation in space, during which the instrument diffuser has degraded by more than 30 percent at the total ozone wavelengths. More details on the Dobson comparison appear in Section 7.5. More details on the calibration procedure are in Section 5.4.

Data quality flags are provided with the derived ozone on the HDTOMS (Level 2) data product. Data quality flag values of 0, 1, and 2 are recommended for use and have been used

to compute the averages provided on the Gridded TOMS (Level 3) product. Larger values indicate retrieved ozone values that are not of good quality.

3.4 Archived Products

Two kinds of TOMS total ozone tape products are archived at the National Space Science Data Center: the High Density TOMS (HDTOMS) tape and the Gridded TOMS Tape (GRIDTOMS). The HDTOMS contains detailed results of the TOMS ozone retrieval for each instantaneous field of view (IFOV) in time sequence. Each HDTOMS Tape contains 3 weeks of data (6.3 megabytes/day). The GRIDTOMS contains daily averages of the retrieved ozone, effective surface reflectivity, and time of measurement in a 1-degree latitude by 1.25-degree (nominal) longitude grid. In areas of the globe where orbital overlap occurs, the most nadir view of a given grid cell is used, and only good-quality retrievals are included in the average. Each GRIDTOMS Tape contains one calendar year of daily TOMS maps (0.4 megabyte/day). Detailed descriptions of these tape products are provided in Section 9, Tape Formats.

In addition to the traditional tape products, TOMS data have now been put on CD-ROM for distribution by the NSSDC. Three CDs are now available: two contain daily-average TOMS ozone in a uniform 1-degree latitude by 1.25-degree longitude grid over the entire globe for the periods 1978 - 1988 and 1989 - 1991 respectively; the third contains image files of the daily maps along with PC display software for the period 1978 - 1991. Additional CDs containing the remainder of the Nimbus-7 TOMS data set may be produced and archived in the near future.

SECTION 4

THEORETICAL FOUNDATION

To interpret the radiance measurements made by the TOMS instrument requires an understanding of how the Earth's atmosphere scatters ultraviolet radiation as a function of solar zenith angle. Incoming solar radiation undergoes absorption and scattering in the atmosphere by atmospheric constituents such as ozone and aerosols, and by Rayleigh scattering. Radiation that penetrates to the troposphere is scattered by clouds and aerosols, and radiation that reaches the ground is scattered by surfaces of widely different reflectivity. The two shortest wavelengths chosen for use in the TOMS ozone measurements were selected because of their high ozone absorption (Table 6.1). At these wavelengths, absorption by other atmospheric components is negligible compared to that of ozone.

The backscattered radiance at a given wavelength depends, in principle, upon the entire ozone profile from the top of the atmosphere to the surface. At wavelengths longer than 310 nm, however, the backscattered radiance consists primarily of solar radiation that penetrates the stratosphere and is reflected back by the dense tropospheric air, clouds, aerosols and the Earth's surface. Because most of the ozone is in the stratosphere, the principal effect of total atmospheric ozone is to attenuate both the solar flux going to the troposphere and the component reflected back to the satellite. This separation of the absorbers in the stratosphere (i.e., ozone) and the "reflector" in the troposphere (i.e., atmospheric scattering, clouds and Earth surface) causes backscattered radiances longer than 310 nm to depend very weakly on the vertical distribution of ozone in the stratosphere.

Derivation of atmospheric ozone content from measurements of the backscattered radiances requires a treatment of reflection from the Earth's surface and of scattering by clouds and other aerosols. In general, the scattered or reflected light depends on both incidence angle of the sunlight and viewing angle of the satellite. Studies by Dave (1978) show that, in practice, the contribution of clouds and aerosols to the backscattered intensity can be treated by assuming that radiation is reflected from a particular pressure level called the "scene pressure," with a Lambert-equivalent "scene reflectivity" R. In addition, then, to deriving a reflectivity for the albedo calculations, a pressure level for the effective reflecting surface must be defined for each instantaneous field of view (IFOV).

The calculation of albedos follows the formulation of Dave (1964) except that a spherical correction has been added for the incident beam. Consider an atmosphere bounded below by a Lambertian surface of reflectivity R. For unit solar irradiance incident at a solar zenith angle of θ_o, the intensity I of the radiation scattered toward zenith angle θ can be expressed as

$$I(\theta,\theta_o,\phi,R,\tau) = I_o(\theta,\theta_o,\phi,\tau) + RI_s(\theta,\theta_o,\tau)f_1(\tau,\theta)/[1-Rf_2(\tau)] \quad (1)$$

where ϕ is the angle between the incident and scattered radiation at the field of view. The two terms on the right-hand side represent the atmospheric and surface contributions to the backscattered radiation, respectively. I_o is the intensity of radiation backscattered from the atmosphere; it represents the intensity that would be observed at zero reflectivity. I_s is the

intensity of direct and diffuse radiation reaching the surface, f_1 is the fraction of reflected radiation emanating from the atmosphere toward zenith angle θ, and f_2 is the fraction of reflected radiation scattered back to the surface. These theoretical intensities are computed for use in the retrieval algorithm described in Section 6.

SECTION 5

INSTRUMENT

5.1 Description

The Total Ozone Mapping Spectrometer (TOMS) on board the Nimbus-7 satellite provides daily global coverage of the Earth's total ozone by measuring backscattered ultraviolet sunlight. TOMS maps total ozone by scanning through the subsatellite point in a direction perpendicular to the orbital plane. The TOMS instrument has a single, fixed monochromator, with exit slits at six near-UV wavelengths. The slit functions are triangular with a nominal 1-nm bandwidth. The order of individual measurements is determined by a chopper that rotates over the exit slits. As the chopper rotates, openings in it pass over the exit slits, allowing measurements at the different wavelengths in an order that is not one of monotonically increasing or decreasing wavelength. Table 5.1 lists the six TOMS wavelength channels, giving the wavelengths determined from the prelaunch calibration. The instrument instantaneous field of view (IFOV) is 3° x 3°. A mirror scans perpendicular to the orbital plane in 3° steps from 51° on the right side of spacecraft nadir to 51° on the left (relative to direction of flight), for a total of 35 samples. At the end of the scan, the mirror quickly returns to the first position, not making measurements on the retrace. Eight seconds after the start of the previous scan, another begins. Consecutive cross scans overlap, creating a contiguous mapping of ozone.

To measure the solar irradiance, a ground aluminum diffuser plate is deployed to reflect sunlight into the instrument. This diffuser plate is shared with the Solar Backscatter Ultraviolet (SBUV) experiment. It is normally deployed once a week for TOMS solar irradiance measurements, in addition to the SBUV deployments.

The TOMS scanner has four operating modes, which determine data processing sequences and data formats:

1. Normal scan mode.
2. Single step mode.
3. View diffuser mode.
4. Stowed mode.

The primary operating mode of the TOMS is normal scan mode. It is in this mode that the scanner scans the 35 scenes corresponding to the scanner view angles. These measurements of backscattered Earth radiance are used to obtain the radiances from which albedos are derived. Solar irradiance measurements are made in view diffuser mode. The scanner moves to the view diffuser position and stops. Wavelength calibration occurs in stowed mode. The scanner slews to the stowed position and stops. The mercury-argon lamp is turned on and the diffuser plate is deployed to reflect light from the lamp into the instrument. Wavelength calibration is

discussed in greater detail in the following section. Heath *et al.*, (1975) provide a more complete description of the instrument and its calibration, along with a diagram of the system. Additional details and descriptions of the other modes are in the RUT User's Guide (Fleig *et al.*, 1983).

5.2 Wavelength Calibration

The TOMS prelaunch wavelength calibration was determined using a photographic technique wherein the positions of the images of the back-illuminated TOMS exit slit were compared to the positions of the spectral-line images of a low-pressure mercury lamp that was placed at the exit slit. The wavelengths in Table 5.1, determined from prelaunch calibration results, have an estimated accuracy of $\pm$0.05 nm.

The purpose of in-orbit wavelength calibration is to detect any change in the wavelengths since the prelaunch calibration. Such change might be produced by excessive temperature differentials or mechanical displacement of the wavelength-determining components resulting from shock, vibration, or wear. Scans of the mercury-argon lamp for in-flight monitoring of the wavelength calibration are normally made about twice a week. TOMS wavelength calibration monitoring uses observations of four wavelength bands, near the center and in the wings of the 296.7-nm Hg line. No detectable change in the wavelength scale has been observed in the first 14 years of flight; the uncertainties in the determination yield an upper limit of 0.005 nm to any possible change, or a possible error in ozone of about 0.2 percent.

5.3 Goniometric Calibration

As the Nimbus-7 satellite orbits the Earth during the solar irradiance measurement, the solar radiation's angle of incidence on the diffuser plate changes. Accurate measurement of the absolute solar irradiance therefore requires calibration of the diffuser's angular reflecting, or goniometric, characteristic. In contrast to SBUV, where individual values of the solar irradiance are necessary for ozone profile determination and where long-term solar spectral irradiance monitoring is one of the instrument's primary goals, the TOMS instrument is not intended to monitor solar irradiance and uses the ratios of irradiances for pairs of wavelengths in the total ozone determination. Therefore, the goniometric accuracy requirements for TOMS are less stringent than those of SBUV; in particular, a wavelength-independent error in the goniometric calibration will not affect these ratios. The TOMS goniometric calibration was derived using in-flight measurements of 380.0-nm solar irradiance (in contrast, the SBUV goniometric characteristics were measured before launch and then checked using in-flight data). At this wavelength, the Sun is essentially constant. The radiation originates at the photosphere, and should vary with time in the same way as the total solar irradiance, although, in the blackbody approximation, the changes may be one and a half times as large. Solar constant measurements by Willson (1982) show a long-term change no greater than 0.1 percent and short-term changes no greater than 0.3 percent over a few days. When the exact goniometric calibration and correction for instrument degradation are applied, TOMS measurements should show no variation within an orbit and should show no systematic seasonal variation. Data from the second and third years of instrument operation were used in the TOMS goniometric calibration. Because of the limitations of the technique, the derived TOMS goniometric calibration contains a small,

wavelength-independent residual error that is manifested as an approximate 0.5-percent peak-to-peak yearly cycle in the derived TOMS solar irradiances. Goniometric errors produce an annual cycle in the data because the position of the Sun at mean noon varies over the year in a manner described by the equation of time, and consequently, the incident angle of the Sun also varies. Because the TOMS total ozone determination uses the ratios of albedos calculated at pairs of wavelengths, the small residual wavelength-independent goniometric error should affect the accuracy of the TOMS total ozone measurement by no more than a few tenths of a percent.

5.4 Albedo Calibration

The TOMS albedo calibration is applied through the use of the Albedo Calibration Factor (ACF). The definition of the ACF is best understood by seeing how it is used. For use in the TOMS retrieval algorithm (described in Section 6), the measured albedo is expressed in the logarithmic form of N-value such that:

$$N(t) = -100 \log \left[\left(\frac{I_m(t)}{F_o} \right) ACF(t) \right] \tag{2}$$

where:

$I_m(t)$ = Earth radiance counts * prelaunch calibration * gain

F_o = day 1 solar counts * prelaunch calibration * gain * g (α,β).

The day-1 solar flux (F_o), prelaunch calibration constants and gain range ratios for TOMS are given in Table 5.1. TOMS measured solar flux (F_m) and Earth radiance (I_m) can be written as:

$$F_m(t) = F_o \, f_{true}(t) \, f_{inst}(t) \, f_{diff}(t) \, g(\alpha,\beta) \tag{3}$$

$$I_m(t) = I_{true}(t) \, f_{inst}(t) \tag{4}$$

where the factors:

$f_{true}(t)$ = true changes in solar output
$f_{inst}(t)$ = change in instrument throughput
$f_{diff}(t)$ = change in diffuser reflectivity
$g(\alpha,\beta)$ = angular dependence of diffuser reflectivity
α = solar elevation in spacecraft coordinates
β = solar azimuth in spacecraft coordinates.

The goniometric dependence $g(\alpha,\beta)$ is assumed to be invariant with time. In practice, both I_m and F_m are corrected for Sun-Earth distance. This makes goniometric errors in the ACF easier to detect by removing the known annual variation.

If we define:

$$ACF(t) = \frac{F_o\, f_{diff}(t)}{F_m(t)} \tag{5}$$

then N-value becomes:

$$N(t) = -100 \log\left[\left(\frac{I_{true}(t)\, f_{inst}(t)}{F_o}\right) \frac{F_o\, f_{diff}(t)}{F_o\, f_{true}\, f_{inst}(t)\, f_{diff}(t)}\right]$$

$$N(t) = -100 \log\left[\frac{I_{true}(t)\, f_{inst}(t)}{F_o\, f_{true}(t)\, f_{inst}(t)}\right] \tag{6}$$

$$N(t) = -100 \log\left[\frac{I_{true}(t)}{F_o\, f_{true}(t)}\right]$$

The problem of maintaining the calibration of the TOMS instrument for ozone trend determination then reduces to the determination of f_{diff} the change in the reflectivity of the solar diffuser used during the irradiance measurements for both TOMS and SBUV.

5.4.1 The Exponential Diffuser Degradation Model

In the Version 5 calibration technique, the diffuser degradation for each wavelength (λ) was modeled as:

$$f_{diff}(\lambda) = \exp\,[r(\lambda)E(t)] \tag{7}$$

where E(t) is the total accumulated solar exposure of the diffuser plate in hours, and $r(\lambda)$ are diffuser degradation constants. A detailed description of this technique is available (Cebula *et al.*, 1988). The constants were obtained from SBUV irradiance measurements made in the continuous-scan mode over the time period 15 July 1980 to 17 September 1981. Included in this time period are two intervals, lasting a total of 206 days, during which substantial diffuser degradation occurred as a result of an accelerated deployment schedule of the solar diffuser. The changes in solar exposure rates of the diffuser during this period allowed the use of a multiple linear regression technique to separate the time dependence and exposure dependence of the instrument changes and to determine the diffuser degradation constants. The exponential model was then used to compute ACF(t) based on the measured solar irradiance and the accumulated

exposure of the diffuser plate. This method was very accurate over the fitted period, but SBUV and TOMS began to show significant drifts relative to the ground-based Dobson network (Fleig *et al.*, 1986a, 1986b), and it was eventually demonstrated that the technique did not provide a unique determination of the diffuser degradation (Watson and the Ozone Trends Panel, 1988). Results from the subsequent Pair Justification Method (PJM) described below indicate that the diffuser degradation is better modeled as a linear function of solar exposure.

5.4.2 The Pair Justification Method

The 1988 Ozone Trends Panel report found the Version 5 Nimbus-7 SBUV and TOMS total column ozone trends from 1979 to 1987 to be a negative 3.5 percent greater than those from the Dobson measurements. The panel concluded the SBUV and TOMS trends were in error due to unaccounted degradation of the instruments' diffuser. Since this finding, the Pair Justification Method (PJM) has been developed to estimate and correct the diffuser calibration drift for both the Nimbus-7 TOMS and SBUV total ozone. The TOMS data have been reprocessed and released as Version 6 data (Herman *et al.*, 1991). This section gives a short overview of PJM, which fundamentally uses a validation procedure based on SBUV measurements to estimate the drift in the Version 5 diffuser calibration.

The SBUV instruments measure Earth radiance and solar irradiance at 12 channels. Like TOMS, the directional albedos (radiance/irradiance) from the four longest wavelength channels (313, 318, 331, and 340 nm) are paired to derive total column ozone. The shorter wavelength channels (255 through 306 nm) are, in general, used to derive profile ozone. A pair of channels is sensitive to total ozone because of the relatively large difference in the pair's ozone absorption. In general, the A-pair (313 and 331 nm) is the predominant pair for total ozone retrieval. At higher solar zenith angles and higher total column ozone, the B-pair (318 and 331 nm) becomes predominant, and at very high solar zenith angles, the C-pair (331 and 340 nm) is predominant.

The Pair Justification procedure, uses a new pair, the D-pair (306 and 313 nm) constructed from the SBUV channels. In general, the 306-nm channel is a profile channel. However, at low total column ozone and small Sun angles, 306 nm "sees" the same column ozone as the operational pairs (A, B, and C). Pair Justification is based on a particular comparison of D versus A-pair albedos (see Herman *et al.*, 1991). Analytical leverage for the procedure exists because the D-pair has significantly higher ozone sensitivity than the A-pair, yet it is less sensitive to wavelength-dependent calibration drift than the A-pair due to its smaller wavelength separation. Assuming a calibration drift that is linear in wavelength for example, the D-pair would be almost five times less sensitive to calibration error than the A-pair. This differential sensitivity along with an assumption about the wavelength dependence of the calibration drift can be used to calculate a calibration correction. Because of the lack of sensitivity of the D-pair to calibration drifts, the result is only weakly dependent on the assumed wavelength dependence.

In February 1987, the SBUV instrument began to have synchronization problems and could no longer be used to derive calibration using PJM. Since TOMS does not have a 306-nm channel, the Pair Justification Method is applied using the A-pair and B′-pair (318 and 340 nm). When the B′-pair is used, however, there is a stronger dependence on the assumed wavelength dependence. As a consequence, the wavelength dependence parameter used in the TOMS calculation was adjusted slightly to normalize the TOMS A-B′ calibration result to the SBUV A-

D result at the end of 1986. Error estimates indicate that the resulting long-term calibration is good to ± 1.3 percent in total ozone over the first 12 years of TOMS data at the 95-percent confidence level.

Since PJM is applied to the Version 5 data, this result represents an adjustment to the diffuser degradation estimates based on the exponential model described in the previous section. The total diffuser degradation is the sum of the degradation predicted by the exponential model and the additional degradation estimated using PJM. Figure 5.1 shows the total diffuser degradation at the 312.5-nm and 331.2-nm channels as a function of accumulated exposure time from November 1978 through January 1989. A linear fit to the last 2 years (about 200 hours) of this type of data has been used to compute coefficients at each wavelength used to predict f_{diff} based on exposure time in the calculation of ACF(t).

$$f_{diff}(t)=A + B\ E(t) \tag{8}$$

The coefficients used are given in Table 5.2. The accuracy of this prediction is found to be better than 1 percent based on re-application of PJM to the extended data set. Comparisons of the processed data with the world standard Dobson instrument number 83 presented in Section 7.5 confirm this finding.

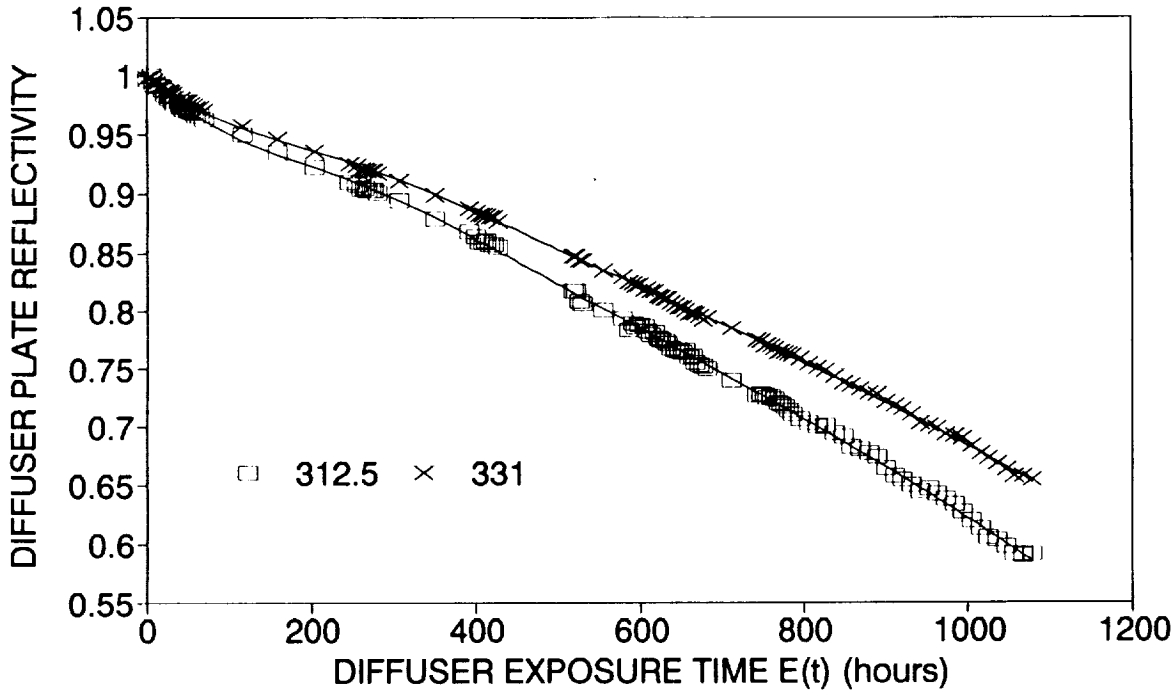

Figure 5.1. Total diffuser degradation as a function of accumulated solar exposure.

TABLE 5.1. TOMS Prelaunch Calibration Constants and Gain Range Ratios.

(for Gain Range 1)

Vacuum Wavelength (nm)	Day-1 Solar Flux at 1A.U. ($W\text{-}cm^{-2}\text{-}cm^{-1}$)	Radiance ($W\text{-}cm^{-2}\text{-}cm^{-1}ster^{-1}\text{-}count^{-1}$)	Irradiance ($W\text{-}cm^{-3}\text{-}count^{-1}$)
380.014	1109.31	2.971×10^{-4}	1.674×10^{-3}
359.962	1126.94	3.309×10^{-4}	1.871×10^{-3}
339.861	994.82	3.381×10^{-4}	1.932×10^{-3}
331.253	972.21	3.483×10^{-4}	2.001×10^{-3}
317.512	786.98	3.731×10^{-4}	2.155×10^{-3}
312.514	662.34	3.995×10^{-4}	2.314×10^{-3}

Gain Range Ratios

Range 2/1	Range 3/2	Range 4/3
6.6	7.2	7.24

TABLE 5.2. TOMS Diffuser Degradation Constants.

Wavelength (nm)	Diffuser Degradation Constants	
	A	B
380.0	1.0301	-2.2889×10^{-4}
360.0	1.0415	-2.8247×10^{-4}
339.9	1.0444	-3.3610×10^{-4}
331.3	1.0483	-3.6428×10^{-4}
317.5	1.0544	-4.1462×10^{-4}
312.5	1.0566	-4.3387×10^{-4}

SECTION 6

ALGORITHM

6.1 Albedos

Albedo measurements are available for the 6 wavelengths listed in Table 5.1. For application of the algorithm, the measured albedos, corrected for instrument sensitivity variations in the way described in Section 5, are converted to the N-Value, defined as follows:

$$\text{N-Value} = -100 \log_{10}(I/F). \tag{9}$$

As discussed in Section 4, theoretical albedos are calculated by a process that uses successive iterations of the radiative transfer equation (Dave, 1964) with the addition of a spherical correction for the incident beam. This calculation requires the following information:

a. Ozone absorption coefficients as a function of temperature for the TOMS wavelengths.

b. Rayleigh atmospheric scattering.

c. Climatological temperature profiles.

d. Climatological ozone profiles.

e. Pressure at the reflecting surface.

f. Solar zenith angle.

g. Satellite zenith angle at the IFOV.

h. Angle between the solar vector and the TOMS scan plane at the IFOV.

The resultant albedos are stored in the tables.

Because of the finite bandwidth of the TOMS measurement, an effective ozone absorption coefficient is used in the calculation of the tables. An integral of measured absorption coefficients across the TOMS slit function, is employed in an iterative technique, which takes into account the variation in atmospheric absorption across the slit due to the presence of ozone (Klenk, 1980). Measurements of the ozone cross-section by Paur and Bass (1985) were used along with measured temperature coefficients, which were assimilated using a simple band average. Table 6.1 gives the ozone absorption coefficients at 0°, and the Rayleigh scattering coefficients the regression equations used for the temperature dependence. Using these functions and standard

temperature profiles (Environmental Science Services Administration *et al.*, 1966 and Appendix C), the altitude dependence of the ozone absorption coefficients at the TOMS wavelengths can be derived. Twenty-three standard ozone profiles have been constructed, from an ozone climatology based on Version 4 SBUV results for altitudes above the 16-mbar level and on balloon ozonesonde measurements for lower altitudes (Bhartia *et al.*, 1985). Each standard profile represents a yearly average for a given total ozone and latitude. Profiles are constructed for three latitude bands: low latitude (15°), mid-latitude (45°), and high latitude (75°). Standard profiles are calculated for total ozone values from a minimum of 225 matm-cm to a maximum of 325 matm-cm from low latitudes and from 125 matm-cm to 575 matm-cm for middle and high latitudes. Given the wavelength, total ozone and ozone profile, surface pressure, and the total optical path, the quantities I_o, I, f_1, and f_2 of equation (1) can then be calculated. For the tables used in the algorithm, these terms are computed at the TOMS wavelengths for all 23 standard profiles and two reflecting surface pressure levels (1.0 atm and 0.4 atm). For each of these cases, I_o and I_s are calculated for ten choices of solar zenith angle, with a finer grid for higher zenith angles. The parameters f_1 and f_2 do not depend on zenith angle.

TABLE 6.1. Absorption and Scattering Coefficients.

Vacuum Wavelength (nm)	Effective Ozone Absorption Coefficient (atm-cm^{-1}) at 0°C (C_o)	Temperature Dependence Coefficients C_1	C_2	Rayleigh Scattering Coefficient (atm^{-1})
312.514	1.8395	5.4325×10^{-3}	2.8943×10^{-5}	1.0206
317.512	0.97759	3.0816×10^{-3}	1.8148×10^{-5}	0.9535
331.253	0.16575	7.2242×10^{-4}	3.9115×10^{-6}	0.7958
339.861	0.03612	3.7546×10^{-4}	2.7186×10^{-6}	0.7137
359.962	$<10^{-8}$	-	-	0.5593
380.014	$<10^{-8}$	-	-	0.4455

Correction to ozone absorption for temperature:

Ozone absorption = $C_o + C_1T + C_2T^2$
(where T is in degrees C)

6.2 Reflectivity

The contribution of clouds and aerosols to the backscattered intensity is treated by assuming that radiation is reflected with a single effective reflectivity from a particular pressure level. In the TOMS ozone retrieval algorithm, the reflectivity for each scan is derived from the radiances measured at the two longest TOMS wavelength positions, 360 nm and 380 nm. At these wavelengths, reflectivity is not sensitive to the ozone amount, so solving (1) for reflectivity R gives:

$$R = (I - I_o)/[I_s f_1 - f_2(I-I_o)] \tag{10}$$

With I_o, I_s, f_1, and f_2 from the tables for the respective wavelengths, reflectivities at surface pressure levels of 1.0 atm and 0.4 atm are computed for both wavelengths. The adopted reflectivity for each level is the average of the reflectivities at the two wavelengths.

6.3 Estimation of Surface Pressure

In the derivation of ozone values, an average IFOV surface pressure, P_o, is obtained from the cloud-top pressure P_{cloud} and the pressure at the actual ground level $P_{terrain}$ using the following expression:

$$P_o = (1-w)P_{cloud} + wP_{terrain}. \tag{11}$$

The weighting function w is based upon the measured surface reflectivity and on the presence or absence of snow/ice. Snow/ice thickness values from around the globe are collected by the Air Force Global Weather Center and mapped on a polar stereographic projection. These data have been averaged to provide a monthly snow/ice climatology mapped onto a 1° x 1° latitude-longitude grid and used to determine the presence or absence of snow in the TOMS IFOV. A higher reflectivity generally implies greater cloudiness (Eck *et al.*, 1987).

Normally, when neither snow nor ice is known to be present, w is set to unity for $R \leq 0.2$, and decreases linearly to zero as the reflectivity increases from 0.2 to 0.6. For $R \geq 0.6$, w is kept at zero. When there is evidence for snow or ice in the IFOV, it is assumed that, despite the high reflectivity, there is only a 50-percent probability that clouds are present. The effective pressure is then obtained by averaging the value of P_o derived from (11) with the terrain pressure.

The cloud-top pressure is obtained from a climatology based on studies using THIR measurements:

$$P_{cloud}(atm) = 0.3 + 0.15[1-\cos(2 \times lat)] \tag{12}$$

The average terrain heights are those available from the National Oceanic and Atmospheric Administration National Meteorological Center (NOAA/NMC). They are provided in km for 2.5 x 2.5-degree latitude and longitude cells. These heights are converted to units of pressure and interpolated to the TOMS IFOVs to establish the surface pressure at the point on the Earth's surface directly below the satellite.

6.4 Computation of Ozone

When measured and computed albedos are compared in the determination of total ozone, the albedos for individual wavelengths are not compared directly. Albedo ratios called pair values are calculated. A pair value is the ratio of the albedo at a longer wavelength, which is relatively insensitive to ozone, to that for a shorter, ozone-sensitive wavelength. The use of albedo ratios reduces the effect of wavelength-independent uncertainties in the instrument calibration.

As discussed in Section 6.1, the measured albedos are expressed in terms of N-values, which are proportional to the logarithm of the albedo. The logarithm of the ratio of albedos is a difference of N-values. Three pairs are defined:

$$\text{A-Pair} = N_{313} - N_{331}$$
$$\text{B}'\text{-Pair} = N_{318} - N_{340}$$
$$\text{C-Pair} = N_{331} - N_{340}$$

Each of the above N-value differences or pairs is used to derive total ozone. For each pair, four estimates of total ozone are calculated. Values are derived for both 1.0 and 0.4 atm. For each of these pressures, ozone values are derived for the two standard latitudes on either side of the actual latitude of measurement. In deriving an ozone estimate, first a surface reflectivity for the assumed pressure is computed as described in Section 6.2. Then, N-values for the particular measurement geometry and the given latitude and pressure level are computed using the table values of I_o, I_s, and f_2 for both the 1.0 and 0.4 reflecting surfaces. Such N-values are computed for total ozone values at 50 matm-cm intervals in the range appropriate to the latitude, as given in Section 6.1. Interpolation of the measured pair N-value between computed pair N-values for different total ozone amounts yields total ozone values at each standard latitude and pressure. The total ozone values derived for the two pressures are linearly interpolated to the scene pressure estimated using (11). The ozone value for the latitude of the measurements is derived by linear interpolation in latitude between the values for the two surrounding latitudes. Between 15° and the Equator, only the profile set for 15° is used; poleward of 75°, only the 75° profile set is used. An average reflectivity is derived from the reflectivities for the two pressure levels in the same manner and is stored on the tapes.

The derived Best ozone is a weighted average of the total ozone values derived from the A, B′ and C-pairs:

$$\text{Best} = (\Omega_A f_A W_A + \Omega_B f_B W_B + \Omega_C f_C W_C)/(W_A + W_B + W_C) \qquad (13)$$

The adjustment factors f_A, f_B, and f_C have been selected to remove biases between the ozone values derived from different pairs. The adjustment factor between two pairs is derived by comparison of ozone values in the regions where both provide information; near a zenith angle of 45° for the A-and B′-pairs and near 75° for the B′-and C-pairs. By convention, the adjustment f_A for the A pair is defined to be unity. The adjustment factor f_C, which corrects for the bias between the A-and C-pairs, is derived from the measured adjustment factor for the C-pair relative to the B′-pair ($f_{C/B}$) by the expression

$$f_C = f_B f_{C/B} \tag{14}$$

for TOMS, f_B=1.022, and f_C=1.034.

The weights W are derived from the following sensitivity factors:

s_1 = sensitivity of the pair N-value to changes in total ozone ($\partial N/\partial \Omega$).

s_2 = sensitivity of the pair ozone to the wavelength dependence of the effective reflectivity (assumed to be inversely proportional to the separation of the two-pair wavelengths).

s_3 = sensitivity of the pair ozone to the vertical distribution of ozone (assumed to be proportional to s_1 divided by the sensitivity that would be derived using Beer's law if all the radiation were scattered from the ground. The Beer's law sensitivity is proportional to the difference between the ozone absorption coefficients at the two-pair wavelengths).

Using the expression

$$W = s_1^2 s_2^2 s_3^2, \tag{15}$$

the overall weighting factor is then given by the following expression:

$$W = (\partial N/\partial \Omega^4)/\delta\lambda^2 \delta\alpha^2 \tag{16}$$

where $\delta\lambda$ is the separation of the two-pair wavelengths and $\delta\alpha$ is the difference between the absorption coefficients at the two-pair wavelengths.

6.5 Validity Checks

The algorithm contains several validity checks for maintaining data quality. Before measured radiances are accepted for use in ozone determination, the solar zenith angle, satellite attitude, and instrument status are checked to ensure the suitability of the radiances and other geophysical input to the algorithm. This section describes the quality checks performed on the derived reflectivity and ozone to identify invalid ozone values caused by either bad input data that passed preprocessing checks or by limitations of the ozone algorithm.

The computed total ozone for each pair must be within a range that can be derived from the tables. For latitudes below 15 degrees, the range is 0.075 atm-cm to 0.35 atm-cm; between 15 and 45 degrees, the range is 0.075 atm-cm to 0.60 atm-cm; and above 45 degrees, it is 0.075 atm-cm to 0.65 atm-cm. If the derived A- or B′-pair ozone is outside this range, it is set to -999., Best ozone is set to -999., and the error flag is set to 9.

Next, checks are made on the reflectivity. The reflectivity must be no less than -0.05 and no greater than +1.05. If the reflectivity is outside this range, the error flag is set to 8. In addition,

the 380-nm and 360-nm reflectivities are compared. If the two differ by more than 0.10, the quality flag is set to 7. Such differences in the two reflectivities could result from significant departure of the real atmosphere and surface from the algorithmic model.

Each of the derived pair ozone amounts is also checked separately for ozone out of range as in the test for Flag 9. If a pair that is out of range is given significant weight in the best ozone computation, the error flag is set to 5.

If these data pass flags 9, 8, 7, and 5, the air mass s is calculated, where s is given by:

$$s = (\sec \theta_o + \sec \theta). \tag{17}$$

A consistency check is then made between Best ozone and the A, B′, or C pair ozone, depending upon the optical path $s\Omega$. The required consistency depends on: 2.5 percent for optical path < 1.5, 5 percent for optical path from 1.5 to 3.5, and 10 percent for optical path $\geq$3.5. The quality flag is set to 4 if inconsistency exists.

Optical Path	Quality Flag	Pair Used in Flag 4 Consistency Check
1.5	0	A
1.5–3.5	1	B′
3.5	2	C

Data that pass flag 4 are checked for sulfur dioxide contamination. The SO_2 index (SOI) is defined (1985) as follows:

$$SOI = [33.30N_{339.8} - 62.55N_{331.2} + 52.28N_{317.5} - 23.03\ N_{312.5} - 11.6 + 66.1s\Omega - 78.5(s\Omega)^2]/s \tag{18}$$

It is designed to be sensitive to the presence of SO_2 but relatively insensitive to the presence of ozone. For values of $s\Omega$ that are less than 2, the SOI is used to screen the ozone values for sulfur dioxide contamination. If SOI>22 (five standard deviations), the sample is given a flag value of 3. If SOI<22, the sample will be flagged with a value of 3 if the sum of the SOI for any 4 consecutive measurements in a scan including the sample under consideration exceeds 44[1+latitude(°)/90]. For $s\Omega \geq 2$, sulfur dioxide screening is based on the difference between Best and C-pair ozone values. The C-pair is sensitive to total ozone principally at high path length and is not affected by the presence of sulfur dioxide. Data are assigned a flag value of 3 if the quantity (Ω - 1.02fcΩ_c) is larger than 40 for a single sample or if the sum for any four consecutive measurements of a scan including the sample being checked exceeds 80[1+latitude(°)/90].

Data that pass flag 3 are assigned a flag value of 0, 1, or 2 as determined by the optical path $s\Omega$ as tabulated above.

The value 10 is added to a flag value if these data were taken on the descending (north to south) part of the orbit.

SECTION 7

GENERAL UNCERTAINTIES

7.1 Accuracy and Precision of TOMS Albedo

Three separate issues are involved in determining the accuracy and precision of the albedo that is used in the total ozone retrieval from TOMS. The first is that of the initial laboratory calibration. An error in this absolute calibration or in the measured band center wavelength or wavelength baudpass may lead to a zero-point error or bias in the retrieved ozone. The second issue is that of possible changes with time in the instrument sensitivity. An error here will cause a drift with time of the derived total ozone values. Finally, the precision of the derived values for total ozone is governed by instrument noise and atmospheric variability within the fields of view.

The accuracy of the initial albedo derived from TOMS measurements depends on the accuracy of the prelaunch radiance and irradiance calibration constants. These constants depend primarily upon the radiometric accuracy ($\pm$3 percent) of the standard calibration lamp supplied by the National Institute for Standards and Technology (NIST) and, for the radiance calibration contants only, upon the accuracy with which the reflecting properties of NIST-calibrated standard $BaSO_4$-coated diffuser plate are known. However, the ratio of radiance and irradiance calibration constants appearing in equation (8) is not affected by the lamp calibration and is known to be better than $\pm$3 percent.

The accuracy of the long-term albedo calibration relative to the first day of measurement depends primarily upon the accuracy with which changes with time in the properties of the diffuser plate are characterized. Herman *et al.* (1991) describe the methods used to estimate the diffuser degradation. They estimate that the accuracy of the method (described briefly in Section 5.7) is sufficient to provide a 1.3-percent uncertainty (two standard errors) in long-term total ozone trends derived from the first 10 years of TOMS data. A more recent study (Gleason *et al.*, 1993) indicates this accuracy has been maintained through the first 14 years of data. For additional insight gained from comparisons with independent ozone measurements, see Section 7.5.

Finally, the precision of the TOMS albedo measurement, which is limited by the digitization of the instrument output, is better than 0.8 percent at all wavelengths.

In addition to changes in sensitivity, uncertainties in the instrument wavelength scale can lead to uncertainties in the retrieved ozone. The algorithm is based on the assumption that the instrument measures radiances and irradiances at a known wavelength and bandpass. If the wavelengths of measurement are not those specified, then the relation between ozone and backscattered radiation will not be that assumed by the algorithm, leading to an error in the retrieved ozone. As discussed in Section 5.2, it is estimated that the initial TOMS wavelength calibration was known to $\pm$0.05-nm accuracy and that the calibration drifted by less than 0.005 nm over the life of instrument.

7.2 Time-Invariant Errors

Table 7.1 summarizes the estimated uncertainties in the retrieved TOMS ozone. It is important to recognize that the use of a single number to describe a source of uncertainty is an oversimplification. In all cases, the uncertainty in total ozone depends upon the wavelengths used in determining ozone, the uncertainty in the measurement at those wavelengths, and the sensitivity of the retrieved ozone to a change in the albedo at that wavelength. The values in Table 7.1 represent values for the most common conditions.

Some cases where the uncertainty may differ significantly from the values in the table are noted.

The first group shown in Table 7.1 consists of sources of random error. The first line shows the uncertainty in total ozone arising from instrument noise. The second line is the uncertainty arising from the digitization of instrument output. In the second group are errors that do not change with time. The third line in this group shows the error in ozone associated with the uncertainty in the wavelength calibration of the instrument, as discussed in Section 7.1. The fourth line shows the error resulting from the uncertainty in the prelaunch radiometric calibration.

7.3 Input Physics

Calculation of the scattering of atmospheric radiation by ozone and the other constituents of the atmosphere requires a knowledge of the ozone absorption and Rayleigh scattering coefficients. The values used in the algorithm are obtained from laboratory measurements. Any uncertainty in the laboratory values will propagate through the algorithm to produce a systematic error in the derived ozone. The first two lines in the time-invariant error group of Table 7.1 show the effect of the uncertainties in these quantities on derived ozone. In addition, the absorptivity of ozone is a function of the temperature. As the temperature changes, the absorption coefficient may change from that assumed in the algorithm, producing an error in retrieved ozone. The size of this error is shown in the third line of the random error group.

TABLE 7.1. Errors in Retrieved TOMS Ozone.

Source	Error
Random - not applicable to long-term change (typical values; may be larger in winter months or under disturbed atmospheric conditions)	
Instrument noise	<0.5%
Digitization	<0.8%
Atmospheric temperature	1%
Retrieval error	1%
Net (Root sum of squares)	2%
Time Invariant	
Rayleigh scattering	<0.5%
Ozone absorption cross-section	<3%[1,2]
Wavelength calibration	<0.5%
Radiometric calibration	1%
Retrieval error	<1%
Time Dependent	
Radiometric calibration	<0.1%/yr
Wavelength calibration	<0.02%/yr
Atmospheric temperature	0.16%/°K
Tropospheric ozone	0.05%/% change

[1] May be 10% or higher at very high solar zenith angles.
[2] Value for comparisons with non-UV instruments or UV measurements evaluated using different ozone absorption cross-sections.

7.4 Time-dependent Errors

The TOMS instrument sensitivity has changed significantly during over a decade of operation in orbit. There has been a concerted, ongoing effort by NASA's Ozone Processing Team to understand TOMS long-term calibration changes. As discussed in Section 5.7 and again in Section 7.1, the relative radiometric calibration over time of TOMS is accurate to about 1 percent/decade, as indicated in Table 7.1.

At low to moderate solar zenith angles, the TOMS derived total ozone is very weakly dependent on differences between the actual vertical distribution of ozone and the standard profile used to compute the look-up tables. At high solar zenith angles, however, this leads to a significant source of random error (Klenk *et al.*, 1982) indicated as retrieval error in Table 7.1.

Given the combination of long-term decreases in upper level ozone measured by SBUV and Umkehr, and a small increase in solar zenith angle associated with the drift in the Nimbus-7 orbit, this error can be shown to have a time dependence as well. Systematic errors as large as -5 percent/decade may be present at latitudes greater than 70° during Northern Hemisphere winter. We estimate that studies limited to latitudes less than 60° will contain seasonal trend errors of less than 2 percent/decade.Because of this, Version 6 TOMS trends derived at high latitudes should be viewed with caution.

As discussed in Section 7.1, a change with time in the wavelength scale can lead to a drift in the derived ozone. Derivation of such a change in the TOMS instrument is described in Section 5.2; no change could be detected. An upper limit to the possible change, based on the upper limits on possible change in the wavelength calibration appears on the first line under the time-dependent changes of Table 7.1.

Long-term temperature changes may also produce a time-dependent error. As noted in Section 7.3, the ozone absorption coefficient varies with temperature. If there are long-term changes in atmospheric temperature, the actual absorption coefficient may drift systematically with time from the values used in the algorithm, producing an error in derived ozone. This error is the third time-dependent error in Table 7.1.

The fourth time-dependent error in Table 7.1 arises from possible long-term changes in tropospheric ozone. TOMS cannot measure ozone that is hidden from the instrument by thick cloud. In the TOMS algorithm, a climatological tropospheric ozone amount is assumed to be present beneath clouds identified by the reflectivity channel of TOMS. An increase in tropospheric ozone of 10 matm-cm would produce only a 5 matm-cm increase in the total ozone retrieved using TOMS measurements. When the Earth's surface is highly reflective, the sensitivity of the TOMS method to tropospheric ozone improves; thus, the problem of tropospheric ozone is less significant over ice-covered regions such as the Antarctic.

The estimates in Table 7.1 for the errors because of changes in atmospheric temperature and tropospheric ozone are obtained by assuming plausible variations. If independent measurements of either quantity were available, such measurements could be used to correct the ozone values derived from TOMS, thus eliminating the contribution of that factor to the uncertainty in the trend.

7.5 Comparison with Other Total Ozone Measurements

The TOMS Version 6 data have been compared with ground-based measurements made each summer at Mauna Loa using the Dobson Network Standard Instrument No. 83. The measurements from the two instruments are generally coincident to within 100 km in space and 1 hour in time. The TOMS ozone is reduced to account for the altitude difference between the summit of Mauna Loa and TOMS scene. The Dobson data are adjusted to reflect the adoption of the Bass and Paur absorption cross-sections by the Dobson network. Each summer's average difference in percent ozone is plotted versus time in Figure 7.1. These data indicate no significant change in bias between the Version 6 TOMS data and the Dobson Reference Standard Instrument No. 83 (McPeters and Komhyr 1991).

Also shown in Figure 7.1 are comparisons between the Version 6 TOMS data and a Dobson network of 22 selected stations. The stations were selected by a data coverage criterion requiring

homogeneous coverage over the 14-year time period 1979 through 1992. Only direct-Sun Dobson measurements have been used, and the Dobson data have been adjusted to reflect the adoption of the Bass and Paur absorption cross-sections by the Dobson network. No latitudinal selection criterion was applied, but the 22 stations tend to be weighted toward mid-northern latitudes. Only the summer data (1 June-31 August) were used in each yearly mean shown in the figure. This plot indicates the presence of a small downward drift in the Version 6 TOMS bias relative to the selected Dobson network. Other results including all seasons for a 39-station network indicate the possibility of a somewhat larger drift in TOMS of 1.1%/decade ± 1.1%/decade (1 standard error) relative to Dobson (Wellemeyer, *et al.*, 1992). This could result from tropospheric increases in ozone that are only partly measured by TOMS. As indicated in Table 7.1, however, this effect implies changes in tropospheric ozone larger than the change in TOMS-Dobson bias by a factor of 20 (or more for summer only), and is probably not the only effect contributing to this small change in bias. Since the Dobson network is centered largely at mid-northern latitudes, the profile shape error discussed in the previous section may also contribute to a downward change in TOMS bias relative to Dobson. The presence of some small change in the TOMS bias relative to the 39-station Dobson network, and of the 39-station Dobson network relative to the Dobson World Standard is also a possible explanation for this result.

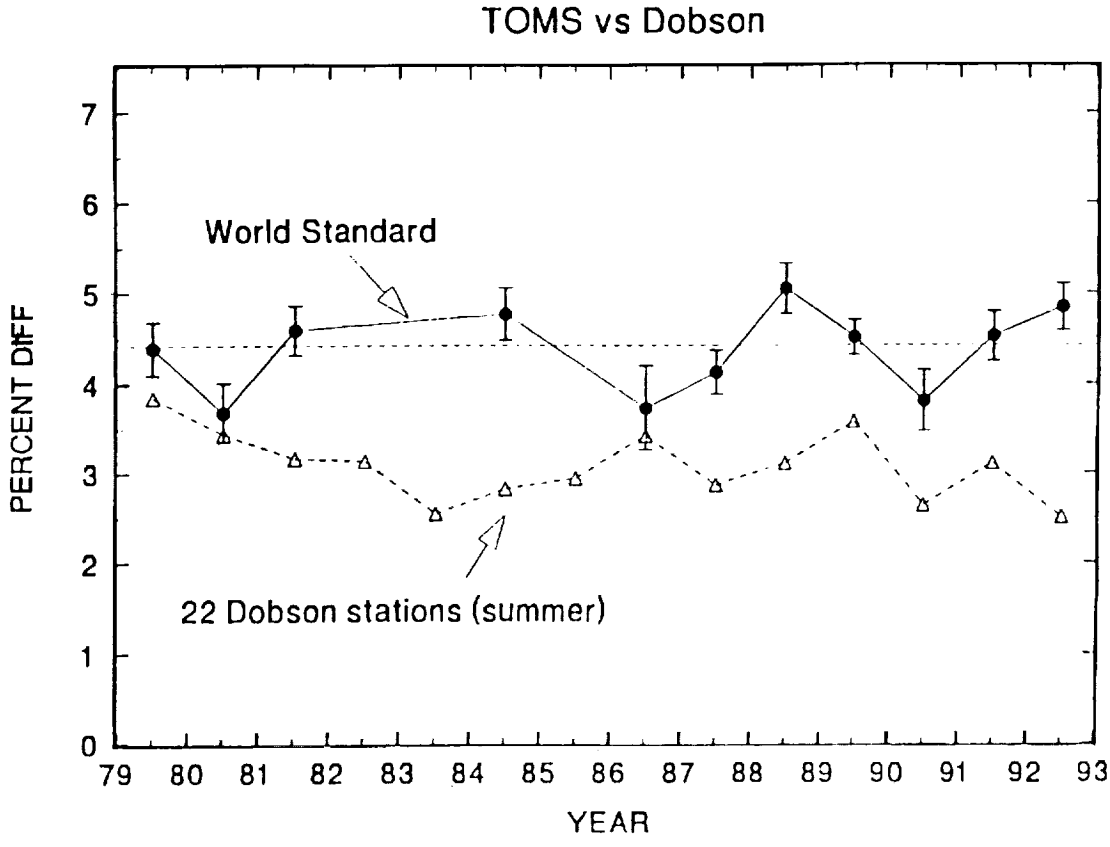

Figure 7.1. TOMS–Dobson comparisons, mean bias summer only.

SECTION 8

PROBLEMS LOCALIZED IN SPACE AND TIME

8.1 Volcanic SO_2 and Aerosol Contamination

The three eruptions of El Chichón in southern Mexico, between March 28 and April 6, 1982, and of Mt. Pinatubo in the Philippines between June 12 and June 16, 1991, injected significant amounts of sulfur-containing gas and dust into the tropical stratosphere. The principal gaseous sulfur compound was SO_2, which changes in time to H_2SO_4 aerosol.

Gaseous SO_2 absorbs in several bands in the 290-nm to 320-nm range. Some bands at longer wavelengths coincide with wavelengths used by TOMS to measure ozone. The effect of this absorption will be to produce a false apparent enhancement in the ozone measured by TOMS after a major eruption. These effects are short lived, because the SO_2 is converted rapidly to sulfuric acid aerosols. Spectral scans of the atmospheric albedo made every 24 days by SBUV show clear evidence of structure attributable to SO_2 on 15 April 1982, a marginally detectable level on 9 May, and no evidence of SO_2 in the albedos for 2 June (McPeters *et al.*, 1984). Following Pinatubo, SO_2 was detectable through at least mid-July, 1991.

When aerosols are present, they may significantly enhance the backscattered radiation at some wavelengths. SBUV spectral scans of Earth radiance show this effect to be most significant at wavelengths shorter than those used by TOMS for the retrieval of total ozone. The impact of any anomalous increase in radiance from the aerosol is further reduced by the use of wavelength pair ratios in the calculation of total ozone. However, following the eruptions of El Chichón and Mt. Pinatubo, anomalies in the TOMS total ozone retrievals became apparent (Bhartia *et al.*, 1993). These anomalies appeared as variations in ozone across the instrument scans that are roughly perpendicular to the orbital motion. They are clearly seen in Figure 8.1 as apparent depressions in the tropical ozone amount near the center of each track (scan positions 18 to 27) and higher ozone values toward the wings of the scan. These effects are of the order of 2 percent. The observed structure is related to the volcanic aerosol scattering-phase function. Figure 8.1 shows zonal scan averages of retrieved ozone after the El Chichón (1982) and Mt. Pinatubo (1991) eruptions. The zonal scan average for 1989 is also shown for comparison. The structure in the 1981 and 1992 dates is related to the aerosol scattering-phase function.

Given the extreme spatial and temporal variability of the effects of volcanoes, it has not been possible to design a retrieval algorithm that removes their effect from the TOMS data. It has, however, been possible to detect the presence of SO_2 in the instrument field-of-view and to flag these data for affected scans. The amount of SO_2 present can be described by the SO_2 index (SOI) defined by equation 18. The SOI was defined in such a way as to be highly sensitive to the presence of SO_2 and relatively insensitive to the presence of ozone. It is used to flag contaminated ozone values, in the manner described in Section 6.4. One unit in SOI corresponds approximately to 1 matm-cm of SO_2. The ozone error that results when SO_2 modifies the backscattered spectrum is, in matm-cm, about half the SOI. The flagging criteria correspond to an estimated error on the order of 11 matm-cm, about 3 to 5 percent, depending on the value of total ozone. In the vicinity of flagged values, SOI values just below the threshold suggest the likelihood of errors that are non-negligible but below the flagging limit. Isolated points with such values could be very localized infusions of SO_2 or noise; they must be evaluated individually.

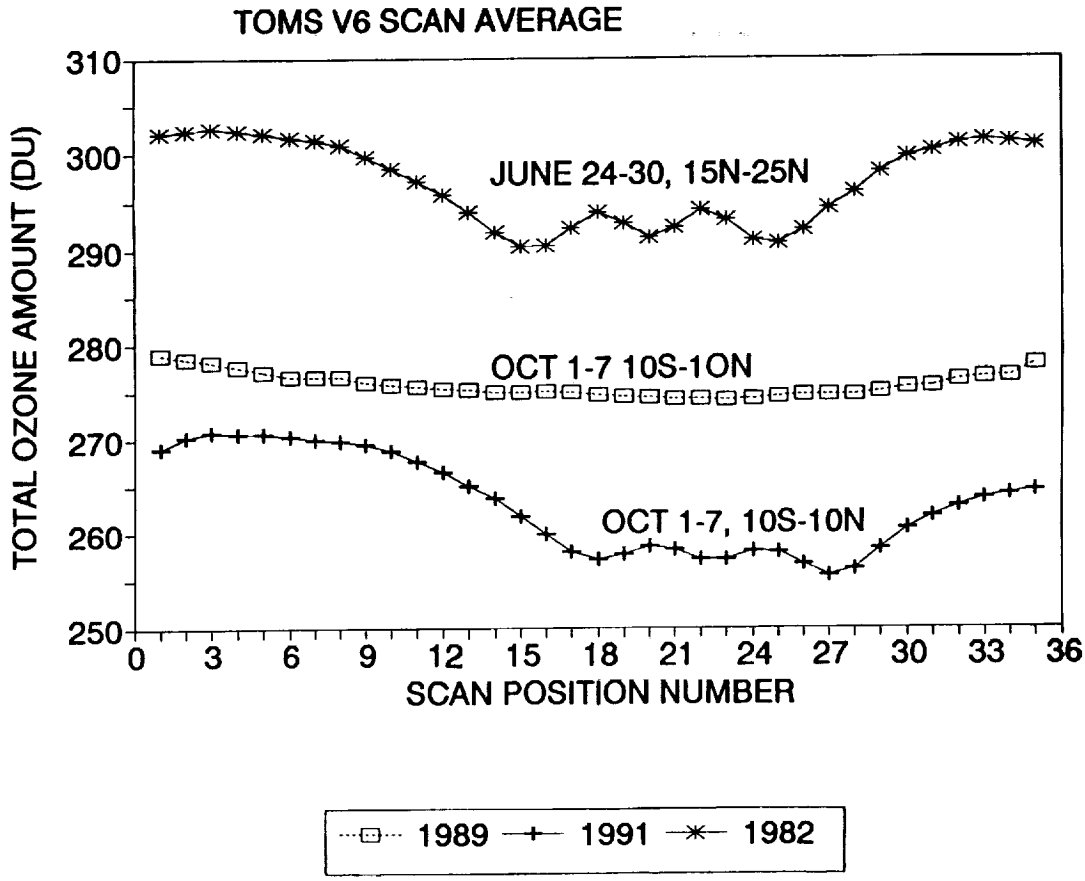

Figure 8.1. Effects of El Chichón (1982) and Mt. Pinatubo (1991) aerosols on TOMS total ozone.

The SOI is packed into the second byte of word 11 of the HDTOMS tape. It does not appear on the GRIDTOMS tape, but HDTOMS values flagged for SOI contamination are not used in the calculations of the ozone averages on the GRIDTOMS tape.

8.2 Instrument Performance Changes Starting April 1984

Instrument Anomalies and the Redefinition of TOMS B-pair Wavelengths

Starting in early 1984, the TOMS instrument began to develop a lack of synchronization between its wavelength selection/chopper wheel and the photon counting electronics (Fleig *et al.*, 1986). This condition is identified by a threshold sensor as "out of synch," and the impact of this condition on the retrieved total ozone has been carefully analyzed. All of the TOMS solar data identified in this way are removed before determining the ACF. Since the onset of non-sync, however, the TOMS has been found to operate in two distinct states, one of which is

normal and the other of which appears to be associated with a sub-threshold non-sync condition. This condition occurs sporadically on short-time scales (less than 1 day) and results in a calibration error in the TOMS albedo, which is computed as the ratio of the measured Earth radiance to the measured solar flux. The solar flux measurements are made over a 5-minute interval during the days on which it is measured, so it is uncertain as to whether a given Earth radiance measurement is made in the same state as the solar flux measurement used to compute the TOMS albedo. The related error in albedo can, therefore, be either positive or negative. The nonsync-related condition (termed toggling) is seen to occur sporadically beginning in 1984 through the present, with a remission during most of 1985. The presence of toggling in the Earth radiance measurements is much more difficult to identify than it is in the solar flux measurements, and no attempt has been made to correct individual measurements for this effect in the Version 6 processing. The impact of toggling on various parameters measured by TOMS is summarized in Table 1. Some wavelengths are more affected by toggling than others; the B′-pair total ozone is less affected by toggling than the B-pair, which was used in the Version 5 processing. As shown in Table 1, the effect of toggling on the B′-pair is only 60 percent of the effect on the B-pair. Because of this, the B′-pair has been used in place of the B-pair in the Version 6 processing. Also, note that the impact of toggling on the C-pair, which is used at very high solar zenith angles, can be quite large.

TABLE 8.1. Impact of Toggling on TOMS Ozone and Reflectivity.

Parameter	Added Noise
Best Ozone (0.75 A-pair + 0.25 B′-pair)	1.0 D.U.
A-pair (312.5 - 331.2 nm)	0.3 D.U.
B′-pair (317.5 - 339.8 nm)	3.0 D.U.
B-pair (317.5 - 331.2 nm)	5.0 D.U.
C-pair (331.2 - 339.8 nm)	13.0 D.U.
Reflectivity	0.003

TOMS radiance measurements that are flagged for non-sync have <u>not</u> been removed from the orbital data used to compute ozone. The non-sync flag is reported on the HDTOMS data set so that these retrievals can be identified, but the non-sync data are included in the averages reported in the Grid-T data set. On balance, the impact of the non-sync condition on the gridded data is probably smaller than the impact of the missing data on the gridded data set if the non-sync data were to be excluded. The daily frequency of occurrence of the non-sync flag is plotted versus time in Figure 8.2. The highest incidence of the non-sync condition was about 90 percent, which occurred during the summer of 1991. The frequency has remained at 20 percent or less during the rest of the period from 1984 to the present (spring 1993). For calendar year 1990, two Grid-T data sets were created; one with all non-sync data included and one with all non-sync data excluded. The standard Grid-T product for all other years includes all non-sync data.

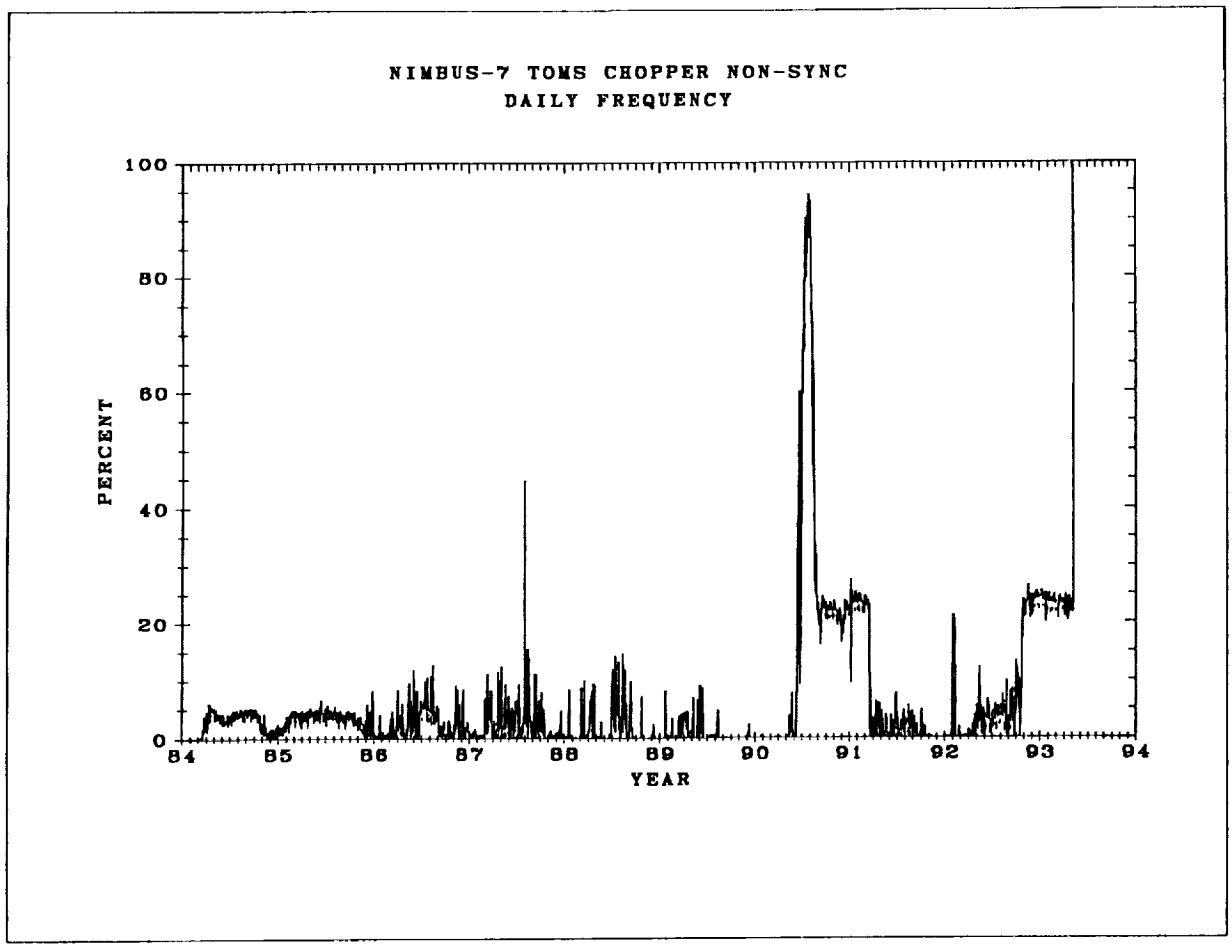

Figure 8.2. Daily frequency of TOMS non-sync flag.

8.3 Solar Eclipses

When the Sun is eclipsed, the decrease in incoming solar irradiance leads to a decrease in the backscattered Earth radiance, as the actual albedo is not affected. However, because the solar irradiance used to calculate the albedo for ozone retrieval is derived from measurements of the uneclipsed Sun, the albedo derived using it will not be correct during times of eclipse. Consequently, ozone values are not retrieved for periods of time and ranges of latitude where the radiances are affected by a solar eclipse. In the actual production, tabulated eclipse information is part of the input stream for the job run and is used by the software to exclude the eclipse periods and regions.

8.4 Polar Stratospheric Clouds

A significant error source that remains in the Version 6 data set is the effect of the presence of anomalously high clouds in the Antarctic region. Polar Stratospheric Clouds (PSCs) above the ozone peak may cause an underestimation of the TOMS retrieved total ozone at large solar zenith angles (larger than 70°). Modeling results indicate that the impact of these clouds on TOMS retrieved total ozone is a strong function of optical depth. Type I PSCs of optical depth 0.01

(composed of $HNO_3/3H_20$, particle mean radius ~.5 μm) may produce an underestimation of up to 2 percent at solar zenith angles greater than 80°. Larger errors (up to 6 percent) may be introduced by Type II PSCs of optical depth 0.05 (water ice, particle mean radius 5~50 μm). Underestimations as large as 50 percent may occur when Type II PSCs of optical depth 0.4 (associated with lee-waves) are present. Errors due to PSCs have not been corrected in Version 6, but tend to be very localized in time and space (Torres *et al.*, 1992).

8.5 Attitude Determination Corrections

Some small errors have been identified in the computation of the Nimbus-7 spacecraft attitude. These errors affect the determination of the viewing geometry associated with each measurement, but they are so small that significant error in total ozone determination occurs only at the extreme off-nadir scan positions, where small errors in spacecraft roll angle affect the path length determined for the backscattered radiation. The identified errors are of the order of 0.1° in roll and correlate both empirically and theoretically with the cross-track bias (of the order of 2 D.U.) observed in the Version 5 TOMS total ozone. The average equatorial cross-track bias has been used along with computed sensitivities to errors in spacecraft roll angle determination to estimate a roll angle correction to the original attitude determination. This indirect method was used in preference to a recomputation of attitude and viewing geometry, which would involve considerable resources. Some evidence of a small latitude dependence in this error was developed, but not taken into account by this approach. The return path length is much less critical at high solar zenith angles, so the associated error in the Version 6 product should be quite small.

8.6 Known Processing Error

A computational error in the derivation of TOMS B′-pair total ozone has been identified, but left uncorrected. Figure 3 summarizes the results of an impact study of this error on TOMS retrieved total ozone. The impact on the derived "best" total ozone is maximum (2 percent) at high reflectivity (100 percent) and low solar zenith angle (mean equatorial conditions). At the modal equatorial reflectivity of 25 percent, the error is less than 1 percent, and at higher solar zenith angles (mid-latitude conditions) even at high reflectivities, the error is less than 1 percent. This error has no time dependence and therefore has no effect on long-term trends derived from the TOMS data. It should be noted however, that this error has been corrected for measurements after July 14, 1990.

SECTION 9

TAPE FORMATS

9.1 High-Density TOMS (HDTOMS) Tape

9.1.1 Overall Structure

The High-Density Total Ozone Mapping Spectrometer (HDTOMS) tape is a 9-track, 6250-bpi tape generated on an IBM 3081 computer under OS/MVS. The first file of the HDTOMS tape is a Standard Header File, which contains a Nimbus Ozone Processing System (NOPS) standard header record, written twice. Following it are the ozone data files. A trailer file and Trailer Documentation File (TDF) follow the last data file. In the more recently processed HDTOMS Tapes, the counter information described in Section 9.1.2 is not accumulated. Figure 9.1 illustrates the structure of an HDTOMS tape.

An HDTOMS tape normally contains 3 weeks of data, for a total of 17-18 tapes for each satellite data year. Each data file on a tape contains data for a single orbit, beginning at the southern terminator. The TOMS instrument generates ozone maps by scanning perpendicular to the orbital plane in 3° steps up to 51° on either side of the orbital plane, a total of 35 samples per scan. Each record contains data for one scan. During each orbit, the TOMS experiment performs approximately 400 scans, for a total of approximately 1.4×10^4 samples for each orbit. Since there are 13-14 orbits each day, each daily map is composed of approximately 2×10^5 samples.

Detailed description of all file types appears in Section 9.1.2.

Tape Specifications

6250 bpi

	Data File and Trailer File	Header File and Trailer Documentation File
Record Format (RECFM)	FB	FB
Logical Record Length (LRECL)	1008 bytes	630
Block Size (BLKSIZE)	16128 bytes	630
Contents character	predominantly binary	character

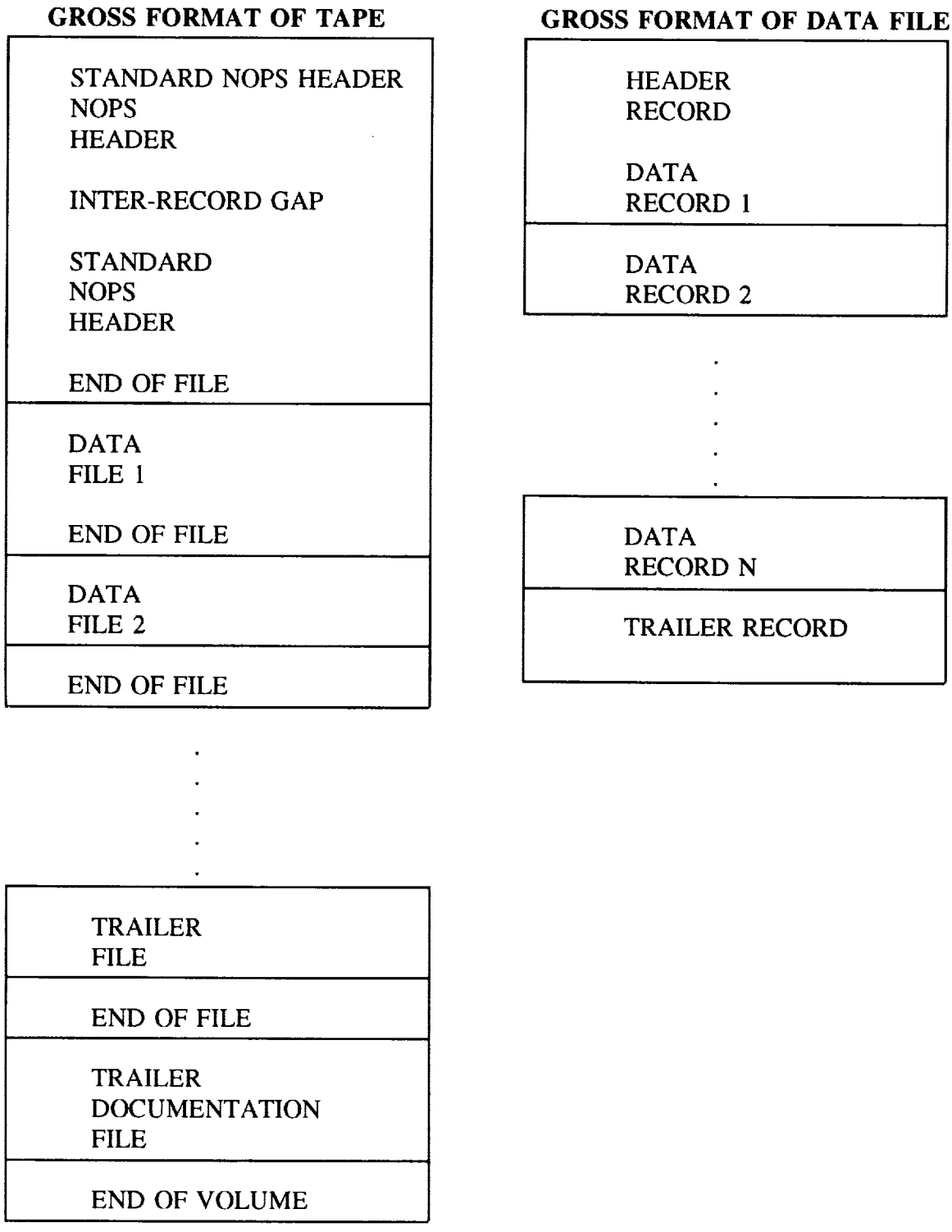

Figure 9.1. HDTOMS tape structure.

9.1.2 Detailed Description

Standard Header File

The Standard Header File contains two identical blocks (physical records) of 630 characters written in EBCDIC. Each block consists of five 126-character lines. Lines 2-5 contain comments about software and data versions. Line 1 is written according to the following standardized format, called the NOPS standard header record.

Line 1:

Columns	Description
1	An indicator to show if a TDF will be found at the end of a tape: blank = No TDF * = TDF present.
2-24	Label: NIMBUS-7$_b$NOPS$_b$SPEC$_b$No$_b$T.
25-30	Tape Specification Number.
31-37	Label: $_b$SQ$_b$NO$_b$.
38-39	Production Definition (PDF) Code: FM for HDTOMS.
40-45	Tape sequence number, defined as follows:
40	The last digit of the year in which these data were acquired.
41-43	Day of year on which the data were acquired (1-366).
44	Used to remove decade ambiguity for character 40. Set to 2 starting 24 October 1988; set to 1 before.
45	Hyphen for the original tape. If there is a remake of the tape for any reason, an ascending alpha character will replace the hyphen.
46	Copy number: 1 = original 2 = copy

HDTOMS Header File

Columns	Description
47	Spare.
48-52	Subsystem ID For HDTOMS: TOMS
53-56	General (source) Facility. For HDTOMS: SACC (Science and Applications Computing Center)
57-60	Label: $_bTO_b$.
61-64	Destination Facility; for derivative products, this is IPD (Information Processing Division, Goddard).
65-87	Start year, day of year, hour, minute, second for data coverage on this tape, in the following form: $_bSTART_b19YY_bDDD_bHHMMSS$.
88-106	End year, day of year, hour, minute, second for data coverage on this tape, in the following form: $_bTO_b19YY_bDDD_bHHMMSS_b$. In order to avoid unnecessary processing complications, the true ending date does not appear in the header record; instead a fill date is used: $1999_b365_b240000$ Tape generation date.
107-126	$GEN_b19YY_bDDD_bHHMMSS$.

$_b$ = blank

See example below.

```
*NIMBUS-7 NOPS SPEC NO T634426 SQ NO FM83041F2 TOMS SACC TO IPD START 1978 304 164738 TO 1999 365 002400 GEN 1990 237 001747
 HIGH DENSITY OZONE(HDOZ) PROG. VERSION 2.0, AUG. 1985
VERSION 6.0 TOMS OZONE CALIBRATION ADJUSTED FOR LONG-TERM DRIFT USING PAIR JUSTIFICATION (FINAL CALIBRATION)
VERSION 6.0 TOMS OZONE CALIBRATION ADJUSTED FOR LONG-TERM DRIFT USING PAIR JUSTIFICATION
 VERSION 6.3 TOMS OZONE SOFTWARE (PROGRAM TOMSALL)              CALIBRATION ADJUSTED FOR LONG-TERM DRIFT USING PAIR JUSTIFICATION
```

Description of First Record on HDTOMS Data Files
Words are REAL*4 Unless Otherwise Noted

Word	Description					
1	Block identifier					
	Bits:	1-12	13-16	17	18	19-24	25-32
		block number on file	spare	1 for last block on file; other-wise 0	1 for last file; other-wise 0	record id (in decimal) 04-first block on data file 19-intermediate blocks on data file 54-last block on data file 57-all blocks on trailer file	spare
2	Logical sequence number: I*2 variable occupying first half of word.						
3	Orbit number.						
4-7	Date of job run (EBCDIC; e.g., MON DEC 10, 1978).						
8	Day of first good scan (sequence number in year: 1-366).						
9	GMT (seconds of day: 1-86400) of first good scan.						
10	Subsatellite latitude (hundredths of a degree) for first good scan of orbit, ranging from -90 degrees (south) to +90 degrees (north).						
11	Subsatellite longitude (hundredths of a degree) for first good scan of orbit, ranging from -180 degrees (west) to +180 degrees (east).						
12	Scan-skipping factor: allows the processing of only every mth scan, where m is the scan-skipping factor. It has not been used in any year of the archived data set (i.e., all scans were processed).						

Description of First Record on HDTOMS Data Files

Word	Description
13	Sample-skipping factor: allows the processing of only every nth sample in each scan, where n is the sample-skipping factor. It has not been used in any year of the archived data set (i.e., all samples were processed).
14	Maximum solar zenith angle processed.
15	Maximum scan angle processed.
16	Minimum subsatellite latitude processed.
17	Maximum subsatellite latitude processed.
18/ 23	Solar irradiance values (watts/cm^3 at 1 a.u.) for the current day at the six instrument wavelengths, in the following order: 380.0 nm, 360.0 nm, 312.5 nm, 317.5 nm, 331.2 nm, 339.8 nm.
24/ 47	Calibration constants.
48	Spare (-77.).
51	GMT of orbit's ascending node (seconds of day).
52	Year at start of orbit (e.g., 1978.).
53/ 252	Spares (-77.).

Content of HDTOMS Data Record

Word	Byte 1	Byte 2	Byte 3	Byte 4
1	Block identifier			
2	Logical sequence number		Day of year at start of scan	
3	GMT (seconds of day) at start of scan			
4	Spare			
5	Chopper synchronization flag		ϕ Angle at sample 1	
6	Latitude		Longitude	
7	Solar zenith angle		(N_A; THIR surface pressure)	
8	Reflectivity		("N_B"; pressure derived from reflectivity)	
9	Total ozone		$\Omega_A/3$	$\Omega_B/3$
10	Ω_{THIR}-$\Omega_{non\text{-}THIR}$ +100	Terrain height	($N_{331.2}$; pressure at physical surface)	
11	$\Omega_C/3$	SOI+100	($N_{339.8}$; snow presence indicator	
12	QUALITY FLAG		($N_{360.0}$-$N_{339.8}$)	($N_{380.0}$-$N_{360.0}$)
13-250	Same as 6 through 12 for samples 2 to 35			
251-252	Spare			

All quantities are written as INTEGER. One-byte words are always positive, with zero indicating missing data. Two- and four-byte words can be either positive or negative with -77 indicating missing data. Other negative values for total ozone indicate bad data. Many quantities are packed together; others have had constants added or multiplied. Detailed descriptions follow.

Detailed Description of HDTOMS Data Record
All Words are INTEGER

Word	Bytes	Description					
1		Block identifier					
	Bits:	1-12	13-16	17	18	19-24	25-32
		block number on file	spare	1 for last data block on file; other-wise 0	1 for last file; other-wise 0	record id (in decimal) 04-first block on data file 19-intermediate blocks on data file 54-last block on data file 59-all blocks all blocks trailer file	spare
2	1-2	Sequence number in file.					
2	3-4	Day of year (1-366) at start of scan.					
3	1-4	GMT at start of scan in seconds (1-86400).					
4	1-4	Spare.					
5	1-2	Flag for chopper non-synchronization occurrence 0: Does not occur in current or next scan. 1: Occurs in current scan, not in next. 2: Occurs in next scan, not current. 3: Occurs in current and next scan.					

Detailed Description of HDTOMS Data Record (Continued)

Word	Bytes	Description
5	3-4	Angle ϕ between Sun and satellite scan plane measured at instantaneous field-of-view (IFOV), in units of 10^{-2} degree.
6	1-2	IFOV latitude, from -90 degrees (south) to + 90 degrees (north), in units of 10^{-2} degree.
6	3-4	IFOV longitude, from -180 degrees (west) to +180 degrees (east), in units of 10^{-2} degree.
7	1-2	IFOV solar zenith angle, in units of 10^{-2} degree.
7	3-4	A-pair N-value, N_A, packed with surface pressure, P_{THIR}, derived from Temperature Humidity Infrared Radiometer (THIR) cloud height information, in the form $10*INT[10*(N_{312.5}-N_{331.2})] + INT[10*P_{THIR}(atm)-0.5];$ e.g., if P_{THIR} =0.925 atm, it is packed as INT (8.75) = 8 (P_{THIR} not used in V6 processing).
8	1-2	Best reflectivity, in percent, obtained from average of 380-nm and 360-nm reflectivities.
8	3-4	N-value for original B pair, "N_B", packed with surface pressure, P_{refl}, derived from reflectivity, in the form $10*INT[10* (N_{317.5} - N_{339.8})] + INT[10*_{refl} - 0.5].$
9	1-2	Best total ozone, using surface pressure derived from reflectivity.

Detailed Description of HDTOMS Data Record (Continued)

Word	Bytes	Description
9	3	A-pair ozone/3, in matm-cm.
9	4	B-pair ozone/3, in matm-cm.
10	1	Not used in V6 processing.
10	2	Estimated difference between total ozone above 1 atm and total ozone above actual terrain pressure, in sense $\Omega_{atm} - \Omega_{terr}$.
10	3-4	331.2-nm N value, packed with pressure (in atmospheres) at ground terrain level, in form $10*INT(10*N_{331.2}) + INT(10*P_{terr} - 0.5)$.
11	1	C-pair ozone/3, in matm-cm.
11	2	100-plus sulphur dioxide index SOI, defined by $SOI = [33.30N_{339.8} - 62.55N_{331.2} + 52.28N_{317.5} - 23.03N_{312.5} - 11.6+66.1s\Omega - 78.5(s\Omega)^2]/s$, where s is the air mass.
11	3-4	339.8-nm N value packed with snow climatology indicator i in form $10*INT[10*(N_{339.8})] + i$ i = 0: snow not present i = 1: snow present.
12	1-2	Data quality flag 0: low path length p = product of air mass and total column ozone $p \leq 1.5$ atm-cm 1: high path length; 1.5 atm-cm $< p \leq 3.5$ atm-cm;

Detailed Description of HDTOMS Data Record (Continued)

Word	Bytes	Description
		2: very high path length;
		3.5 atm-cm < p;
		3: SO_2 contamination: SOI >22 or sum of SOI for any 4 consecutive measurements including a sample that exceeds 44[1+latitude(degrees)/90] (see also Section 6.5);
		4: Ozone value from individual pairs differs from Best ozone by more than following amount: A: 2% for sec z $\leq$ 1.5 B: 5% for sec z $\leq$ 3.5 C: 10% for sec z $\leq$ 3.5;
		5: Ozone out of range for individual weighted pair;
		6: Not used;
		7: Reflectivities at 360 nm and 380 nm differ by more than 0.10;
		8: Reflectivity not within following limits: -0.05<r<1.05;
		9: Ozone not in following range latitude <15°: 125-350 matm-cm latitude 15°-45°: 125-600 matm-cm latitude <45°: 125-650 matm-cm;
		0x: Data from ascending part of orbit (south to north);
		1x: Data from descending part of orbit(north to south).

Detailed Description of HDTOMS Data Record (Continued)

Word	Bytes		Description
	12	3	$INT[10*(N_{360.0} - N_{339.8})] + 100$
	12	4	$INT[10*(N_{380.0} - N_{360.0})] + 100$
	13-19		Same as 6-12 for sample 2.
		20-250	Same as 6-12 for samples 3-35.
		251-252	Spares.

Contents of HDTOMS Trailer Record
Words are REAL*4 Unless Otherwise Noted

Word	Description					
1	Block identifier					
Bits:	1-12	13-16	17	18	19-24	25-32
	block number on file	spare	1 for last data block on file; other-wise 0	1 for last file; other-wise 0	record id (in decimal) 05-first block on data file 20-intermediate blocks on data file 55-last block on data file 61-all blocks trailer file	spare

2 Logical sequence number: I*2 variable occupying first 2 bytes of word; negative of record sequence number in file.

3 Orbit number.

4 Day of last scan on file (1-366).

5 GMT (seconds) for last scan on file (1-86400).

6 Latitude: -90° (S) to +90° (N) for last scan (hundredths of a degree).

7 Longitude: -180° (W) to +180° (E) for last scan (hundredths of a degree).

8 Number of input/output errors for this file.

9 Number of scans read from RUT tape file.

10 Number of scans written on file.

11 Number of good samples written on file (quality flags 0-2 or 10-12).

Contents of HDTOMS Trailer Record (Continued)

Word	Description
12	Number of samples out of range (total).
Number of samples out of range for (13-15)	
13	Zenith angle > 88°.
14	Latitude out of range.
15	Counts out of range (negative).
16	Number of samples written that were bad (total).
Number of samples written that were bad for (17-22)	
17	Ozone out of range (quality flag 9).
18	Best reflectivity out of range (flag 8).
19	$R_{380.0}$ - $R_{360.0}$ difference too large (flag 7).
20-21	Spares.
22	Pair inconsistency (flag 4).
23	Number of large SOI samples (flag 3).
24	Number of good samples, very high path (flag 2).
25	Number of good samples, high path (flag 1).
26	Number of good samples, low path (flag 0).
27-252	Spares.

Format of HDTOMS Trailer File Record
Words are REAL*4 Unless Otherwise Noted

Word	Description					
1	Block identifier					
Bits:	1-12	13-16	17	18	19-24	25-32
	block number on file	spare	1 for last data block on file; other-wise 0	1 for last file; other-wise 0	record id (in decimal) 05-first block on data file 20-intermediate blocks on data file 55-last block on data file 61-all blocks trailer file	spare
2	Trailer file identifier (-1) (first two bytes).					
3	Orbit number of last orbit on tape.					
4	Day of last scan on tape (1-366).					
5	GMT of last scan on tape (seconds: 1-86,400).					
6	Latitude for last scan (hundredths of a degree).					
7	Longitude for last scan (hundredths of a degree).					
8	Number of input/output errors for tape.					
9	Number of scans read from input RUT tapes.					
10	Number of scans written on this tape.					
11	Number of good samples written on tape.					

Format of HDTOMS Trailer File Record (Continued)

Word	Description
12	Number of samples out of range (total).
	Number of samples out of range for (13-15).
13	Zenith angle > 88 degrees.
14	Latitude out of range.
15	Counts out of range (negative).
16	Number of samples written that were bad (total).
	Number of samples written that were bad for (17-22).
17	Ozone out of range (quality flag 9).
18	Best reflectivity out of range (flag 8).
19	$R_{380.0}$ - $R_{360.0}$ difference too large (flag 7).
20-21	Spares.
22	Pair inconsistency (flag 4).
23	Number of samples with large SOI (flag 3).
24	Number of good samples, very high path (flag 2).
25	Number of good samples, high path (flag 1).
26	Number of good samples, low path (flag 0).
27-28	Spare (-77.).
29	Number of files on tape.
30	Number of RUT tapes read in creating this tape.
31-32	YYDDD for first input tape (EBCDIC).

Format of HDTOMS Trailer File Record (Continued)

Word	Description
33-34	YYDDD for second input tape (EBCDIC).
.....	.....
30+2*N	YYDDD for Nth and last input tape (EBCDIC).
31+2*N	Start orbit number.
32+2*N	End orbit number.
33+2*N	RUT IPD history (128 EBCDIC characters).

9.2 GRIDTOMS Tape

9.2.1 Introduction

The Gridded TOMS (GRIDTOMS) contains daily total ozone and reflectivity averages in a latitude-longitude grid. The averages are derived from the individual measurements on the HDTOMS tape. In the averaging process, only data with flags of 0-2 normally are accepted; i.e., all path lengths, no data with probable SO_2 contamination, and no data from the descending (north to south) half of the orbit. The grid interval in latitude is 1°, and the spacing in longitude varies from 1.25° near the Equator to 5° near the poles. Users who are interested in an ozone grid at this or lower resolution and not in the full set of individual scan values will find this tape to be the most useful product.

The gridding scheme used to generate this data set was designed especially for the TOMS ozone data. It meets four basic requirements to satisfy most users:

a. The cell size remains roughly constant throughout the globe.

b. The TOMS resolution is preserved as much as possible.

c. The overall quantity of TOMS data is substantially reduced; a single 6250-bpi GRIDTOMS tape can hold data for 1 year.

d. The grid can be easily converted into other commonly used grid arrays, e.g., ERB grid, NMC grid.

Gridded averages are provided over the globe once a day. The global area is divided into 1° latitude zones. Each zone is subdivided into cells. The number of cells in a zone varies from 288 at the Equator to 72 near the poles, as described in Table 9.1. A set of average values of three quantities for individual orbits, henceforth called the "observational set," is provided for each cell: total ozone, reflectivity, and time of observation. Because the constant separation in degrees between orbits corresponds to a smaller distance in kilometers closer to the poles, a particular cell may be viewed from several adjacent orbits in the higher latitudes. Measurements from adjacent orbits are about 100 minutes apart and can be used to provide information regarding the temporal variability of ozone. For this reason, the grid array is designed to accommodate more than one orbital average or observational set as the orbits overlap in the high latitudes poleward of 50°. The grid is also designed in such a way that the product of the number of cells in a zone times the number of orbital observations permitted per cell is constant (288 slots per zone) over all latitudes (see Table 9.1). The dimension of the data array is thus the same for all latitudes.

For each cell, there is a "primary observational set" of total ozone, reflectivity, and time. Additional observational sets are provided for cells poleward of 50°, as prescribed in Table 9.1. The only criterion used to select an observational set for a cell from several that might be available is the spatial resolution of the TOMS sample. Since the size of the TOMS field-of-view varies from 50 km^2 at nadir to more than 150 km^2 at extreme off-nadir, the observational sets for a cell coming from different orbits will have different spatial resolution. The observational set with the best spatial resolution will be the one closest to sample number 18, the nadir sample; it is the "primary observational set." The rest of the observational sets are ordered by spatial resolution, highest resolution set first. If there are more observational sets for the zone than can be stored on the tape, only those with best resolution will appear on the tape.

Because the size of GRIDTOMS cells varies with latitude and the TOMS sample area varies with the scanning angle, the number of TOMS samples falling into a particular grid cell varies from zero to as many as six, depending on the zone and the suborbital track. For a particular cell with more than one TOMS sample, each sample is weighted by the area that is in both the grid cell and the FOV. Since it is difficult to model the exact shape and orientation of the TOMS FOV, a simplifying assumption is used; the boundaries of the FOV are assumed to lie along lines of constant latitude and longitude. The weighting factor is applied to the total ozone, reflectivity, and GMT time, and is summed separately for each cell. At the end of an orbit, the weighted sums are divided by the sum of the weighting factors to give the area averages.

Each output file represents a single day. Because the map is constructed by gathering data as the satellite sweeps around the globe, there will be a line on the map where data for adjacent grid locations will be nearly 24 hours apart, with data on one side measured near the beginning of the day and data on the other side, near the end of the day. Because of the satellite's noon orbit, this boundary will be near 180° at 0000 GMT, but as the orbit is inclined to the north-south direction, the boundary would be inclined like the orbit itself if each scan were assigned to the day it was made. The daily maps are now constructed so that this boundary falls on the 180° meridian. To implement this decision, the following rule is used: scans at West longitudes are assigned to the earlier day, and scans at East longitudes are assigned to the later day. In the records for a given day, times for data from the previous day will have 24 hours subtracted from the actual time (and be negative); times for data from the next day will have 24 hours added.

TABLE 9.1. Specifications for the GRIDTOMS Grid.

Constant latitude increment of 1.0° from pole to pole (180 zones)					
Latitude	Longitude Size	Number of of Cells in Zone (N)	Number of Observations Permitted per Cell (M)	Expected # of Orbits per Cell	Resolution (km x km)
0°	1.25°	288	1	1.0	110 x 138
to 50°				1.6	110 x 88.4
50°	2.5°	144	2	1.6	110 x 176
to 70°				3.5	110 x 94.1
70°	5°	72	4	3.5	110 x 188
to 80°				7.3	110 x 95.5
80°	5°	72	4	7.3	110 x 95.5
to 90°				14.0	110 x 0.0

9.2.2 Overall Structure

Tape Specifications: 6250-bpi 9-track no-label tape (spec. # 634436)

	Header File	Data Files	Trailer File	*Trailer Documentation File
File Number	1	2 to N+1	N+2	N+3
Physical Record length (blocksize)	630 bytes**	7,056 bytes 56,448 bits	7,056 bytes 56,448 bits	630 bytes
Record format	Fixed block	Fixed block+	Fixed block+	Fixed block
Data Type	EBCDIC	binary	binary	EBCDIC
Number of logical records per block	1	4	4	1
Record ID Number	None	61=data records 62=trailer records	63	None

Requirement Identification: GRIDTOMS Tape Specification Number T634436

Input Data Source: High-density (6250 bpi) HDTOMS tapes.

* Trailer documentation file exists only for tapes with an ' character in the first byte of the NOPS Standard Header in file 1.

** 1 byte=8 bits

+ DCB=(RECFM = FB, LRECL = 1764, BLKSIZE = 7056, DEN = 4)

See Table 9.1 for meaning of tape specification number.

Figure 9.2 shows the order of files on a GRIDTOMS tape. Each data file consists of a single daily map of TOMS data. Averages for neighboring cells come either from the same scan, consecutive scans, or consecutive orbits, except at 180°, across which the GMT of the data differs by about 24 hours. Thus, a particular orbit may be split between two files, depending on the longitude of the samples.

Each GRIDTOMS data file contains 180 logical data records blocked into 45 physical records (blocks); it is then followed by a trailer block of 4 logical records. Each data record contains data for one latitude zone, beginning with the 89°-90° South zone and ending with the 89°-90° North zone. Figure 9.3 shows the order of latitude zone records in a file.

Each logical record in the GRIDTOMS data file represents a 1° latitude zone. There are 882 16-bit (2 byte) integer words in each record. The first 10 words contain header information about the zone; the next 3N words contain the "primary observational set" of time, total ozone, and reflectivity for each of the N cells in the zone. For zones poleward of 50°, the next 3N words contain a set of alternate observations for each of the cells. This pattern repeats M times, where M is the maximum number of permitted observations for each cell in the zone. The first cell contains data from longitude 180°W, extending eastward the number of degrees specified for the latitude in Table 9.1. Successive cells progress eastward, until the last cell is bounded at 180°E. For 50°-70° latitude, for example, the longitude ranges are 180°W-177.5°W,177.5°W-175°W,..., 177.5°E-180°E. The data for a given cell may include data from a day neighboring the date of the file. This neighboring-day data will occur just to either side of 180° and are due to the slight inclination of the orbital track. Data from the previous day will be identified by a negative GMT indicating how long before the given day these data were taken. Data from the next day will have a GMT greater than 24 hours. Figure 9.4 illustrates the GRIDTOMS record structure.

The trailer record marks the end of a data file. It is located in the 46th block of the file and has the file control bit set to 0 and record control bit set to 1. The record ID contains 62 in the IPD word (words 1 and 2 - see Figure 9.5).

Every tape contains a trailer file with only one physical record. The blocksize of the trailer file is the same as that for the data files; it contains a physical record (block) number of 1, a record ID of 63 and the two file control bits set to 1 in words 1 and 2-block identifier. Word 3 contains a special sequence number (-1). The remaining words contain a fill value (-777). The trailer file is used to mark the end of data on the tape.

The trailer documentation file is the last file on each volume (tape). Its structure is the same as the NOPS Standard Header File and contains a collection of Standard Header Files from all input tapes that were used to produce this tape, except that the Standard Header Files are written only once, not twice as they would be at the start of a tape. The trailer documentation file is written in EBCDIC and is used to identify the genealogy of each tape. The first record identifies it as the trailer documentation file.

Chars. 1-10: **********

11-126: NOPS TRAILER DOCUMENTATION FILE FOR TAPE PRODUCT T [Spec. No. (6 digit)] GENERATED ON DDDHHMM.

The second physical record of the trailer documentation file is a repeat of the Standard Header

File for the current tape with a correct end time instead of the fill value on the Header File. Subsequent physical records contain the historical standard header records from the various input tapes.

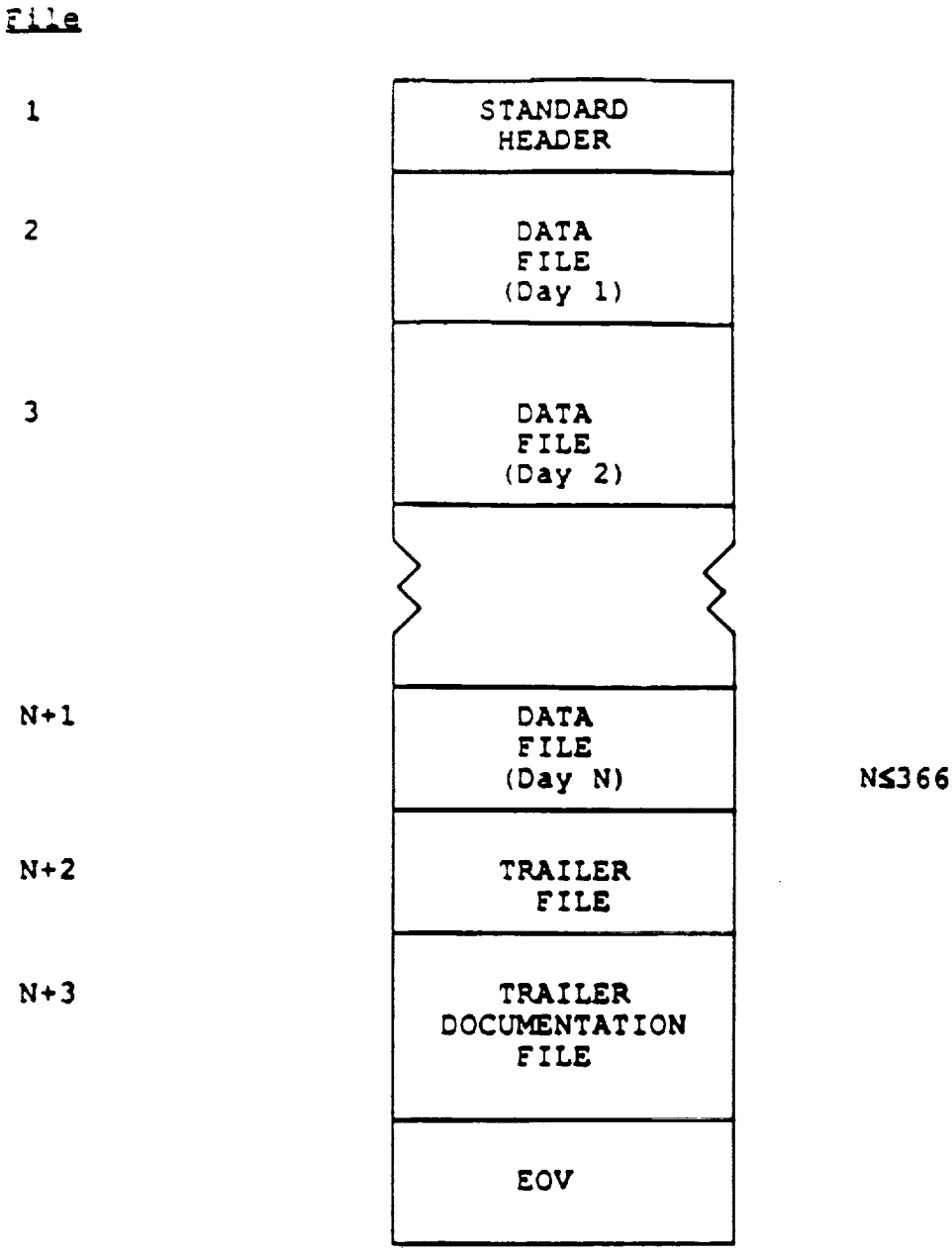

Figure 9.2. GRIDTOMS tape structure.

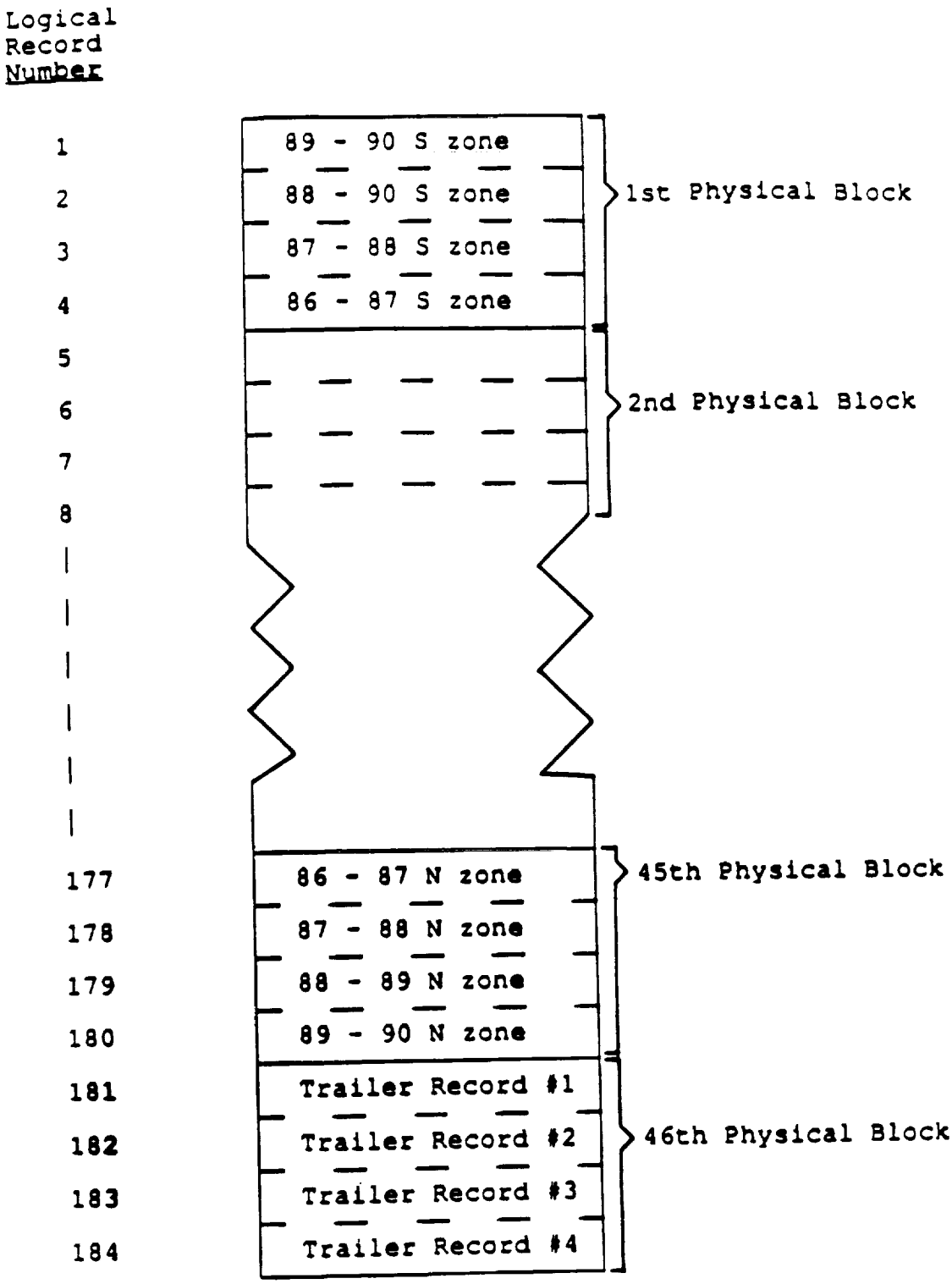

Figure 9.3. GRIDTOMS data file structure.

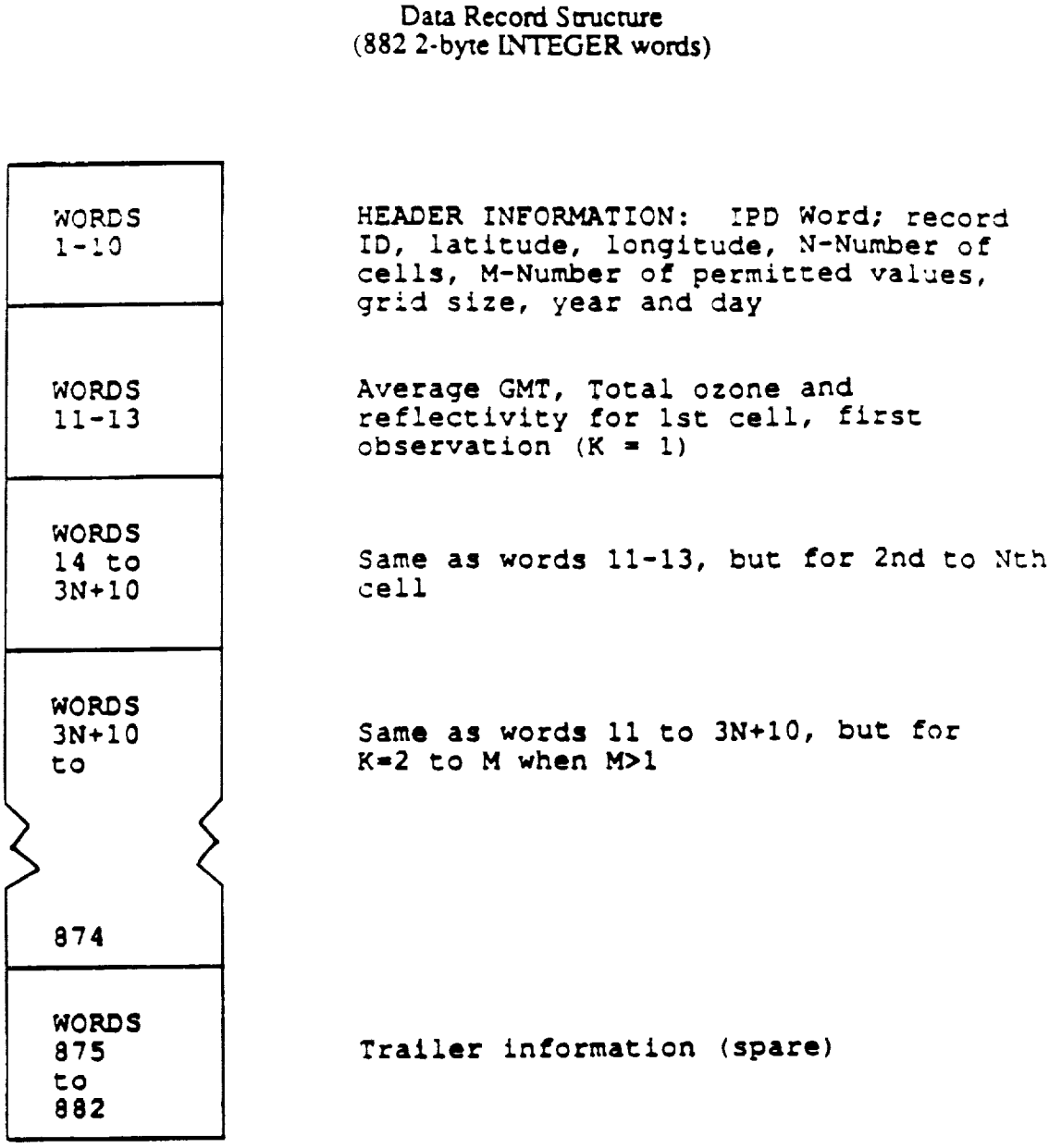

Figure 9.4. GRIDTOMS data record structure.

9.2.3 Detailed Description

Detailed Format of GRIDTOMS Standard Header File

The standard header file contains two identical blocks of 630 characters written in EBCDIC. Each block consists of five 126-character lines. Lines 2-5 contain comments about software and data versions. Line 1 is written according to the following standardized format called the NOPS standard header record.

Line 1:

Columns	Description
1	An indicator to show if a TDF will be found at the end of a tape: blank = No TDF * = TDF present.
2-24	Label: NIMBUS-7$_b$NOPS$_b$SPEC$_b$No$_b$T.
25-30	Tape Specification Number.
31-37	Label: $_b$SQ$_b$NO$_b$.
38-39	PDF Code: FN for GRIDTOMS.
40-45,47	Tape sequence number, defined as follows:
41-43	Day of the year (1-366) in which the data were acquired.
44	Used to remove decade ambiguity for character 40. Set to 2 starting 24 October 1988; set to 1 before.
45	Run version number, represented by an ascending alphabetical character.
46	Copy number 1 = original 2 = copy.
47	Spare.

Detailed Format of GRIDTOMS Header File (Continued)

Columns	Description
48-52	Subsystem ID for GRIDTOMS: TOMS.
53-56	Generation (Source) Facility. For GRIDTOMS: SACC.
57-60	Label:$_b$TO$_b$.
61-64	Destination Facility. For derivative products, this is IPD$_b$ (Information Processing Division, Goddard).
65-87	Start year, day of year, hour, minute, second for data coverage on this tape, in the form $_b$START$_b$19YY$_b$DDD$_b$HHMMSS$_b$.
88-106	End year, day of year, hour, minute, second for data coverage on this tape, in the form TO$_b$19YY$_b$DDD$_b$HHMMSS$_b$ (In order to avoid unnecessary processing complications, the true ending date does not appear in the header record, instead a fill date is used: 1999$_b$365$_b$240000).
107-126	Tape generation date GEN$_b$19YY$_b$DDD$_b$HHMMSS$_b$.

$_b$ = blank

See example below:

```
*NIMBUS-7 NOPS SPEC NO T634436 SQ NO FN83051F2 TOMS SACC TO IPD  START 1978 305 164738 TO 1999 365 002400 GEN 1993 112 183554
 GRIDDED TOMS      VSN 2.9 OCT. 89
  GRIDTOMS VER 2.9   FROM V6 HDT CONTAINING FINAL CALIBRATION    BASED ON PAIR JUSTIFICATION.
```

GRIDTOMS Data Record Format

Word	#Bytes	Type	Description
1-2	2	Packed Integers	IPD Word
3	2	Integer	Record sequence number: 1 to 180 for data file records; -180 for data trailer record; -1 for trailer file.
4	2	Integer	Latitude for center of the 1° zone (in degrees x 10).
5	2	Integer	Longitude for the center of the first cell, (in degrees).
6	2	Integer	Longitude grid size for the zone (in degrees x 100).
7	2	Integer	N, the number of grid cells in the latitude zone.
8	2I	Integer	M, the number of observations permitted per cell.
9	2	Integer	Year (e.g., 1978).
10	2	Integer	Day of the year (e.g., 304).
11	2	Integer	GMT time of the primary observation (best resolution) for the first cell in the zone (in GMT hour x 1000).
12	2	Integer	Total ozone (matm-cm) corresponding to the observation in word 11.

GRIDTOMS Data Record Format (Continued)

Word	#Bytes	Type	Description
13	2	Integer	Reflectivity corresponding to the observation in word 11 (in percent).
13 to 3N+10	2	Integer	Same as words 11 to 13 except for the second to Nth cells in the zone.
3N+11 to 874	2	Integer	Same as words 11 to 3N + 10 except for the 2nd to Mth observations (poorer resolutions) if M > 1 for the zone.
875-2.882	2	Integer	Spare words(-777).

*The IPD words (words 1 + 2) are a 32-bit block identifier with information for Nimbus-7 data tape management and quality control.

MSB PHYSICAL RECORD (BLOCK) NUMBER	SPARE	RECORD CONTROL	FILE CONTROL	RECORD ID	SPARE
(12 Bits)	(4 Bits)	(1 Bit)	(1 Bit)	(6 Bits)	(8 Bits)

Record Control: = 1 if last block on file
File Control: = 1 if last file on tape (trailer file)
Record ID: = 61 for data records; 62 for trailer records; 63 for trailer file records.

Figure 9.5. IPD word format.

REFERENCES

Bates, D. R., "Rayleigh scattering by air," *Planet. Sp. Sci., 32,* 785-90, 1984.

Bhartia, P. K., D. Silberstein, B. Monosmith, and Albert J. Fleig, "Standard profiles of ozone from ground to 60 km obtained by combining satellite and ground based measurements," in *Atmospheric Ozone*, edited by C. S. Zerefos and A. Ghazi, pp. 243-247, D. Reidel, Dordrecht, 1985.

Bhartia, P. K., J. R. Herman, R. D. McPeters, and O. Torres, "The effect of stratospheric aerosols on TOMS ozone measurements," submitted, *J. Geophys. Res.* 98, 1993.

Cebula, R. P., H. Park, and D. F. Heath, "Characterization of the Nimbus–7 SBUV radiometer for the long-term monitoring of stratospheric ozone," *J. Atm. Ocean. Tech., 5,* 215-227, 1988.

Dave, J. V., "Meaning of successive iteration of the auxiliary equation of radiative transfer," *Astrophys. J., 140,* 1292-1303, 1964.

Dave, J. V., "Effect of aerosols on the estimation of total ozone in an atmospheric column from the measurement of its ultraviolet radiance," *J. Atmos. Sci., 35,* 899-911, 1978.

Eck, T. F., P. K. Bhartia, P. H. Hwang and L. L. Stowe, "Reflectivity of Earth's surface and clouds in ultraviolet from satellite observations," *J. Geophys. Res.*, 92(D4), 4287-4296, 1987.

Environmental Science Services Administration, National Aeronautics and Space Administration, and United States Air Force, *U. S. Standard Atmosphere Supplements,* U.S. Government Printing Office, Washington, DC, 1966.

Fleig, A. J., P. K. Bhartia, and David S. Silberstein, "An assessment of the long-term drift in SBUV total ozone data, based on comparison with the Dobson Network," *Geophys. Res. Lett.*, 1359-1362, 1986b.

Fleig, Albert J., Pawan K. Bhartia, Charles G. Wellemeyer, and David S. Silberstein, "Seven years of total ozone from the TOMS instrument—a report on data quality," *Geophys. Res. Lett., 13,* 1355-1358, 1986a.

Fleig, A. J., D. F. Heath, K. F. Klenk, N. Oslik, K. D. Lee, H. Park, P. K. Bhartia, and D. Gordon, "User's guide for the Solar Backscattered Ultraviolet (SBUV) and the Total Ozone Mapping Spectrometer (TOMS) RUT-S and RUT-T data sets, October 31, 1978 to November 1, 1980," *NASA Reference Publication 1112*, National Aeronautics and Space Administration, Washington, DC, 1983.

Fleig, A. J., K. F. Klenk, P. K. Bhartia, and D. Gordon, "User's guide for the Total Ozone

Mapping Spectrometer (TOMS) instrument first year OZONE-T data set," *NASA Reference Publication 1096*, National Aeronautics and Space Administration, Washington, DC, 1982.

Fleig, Albert J., David S. Silberstein, Charles G. Wellemeyer, Richard P. Cebula, and Pawan K. Bhartia, "An assessment of the long term drift in TOMS total ozone data," submitted to *Geophys Res. Lett.*, 1988.

Fleig, A. J., D. S. Silberstein, R. P. Cebula, C. G. Wellemeyer, P. K. Bhartia, and J. J. DeLuisi, "An assessment of the SBUV/TOMS ozone data quality, based on comparison with external data," in *Ozone in the Atmosphere*, edited by R. D. Bojkov and P. Fabian, pp. 232–237, A. Deepak, Hampton, Virginia, 1989.

Gleason, J. F., P. K. Bhartia, J. R. Herman, R. McPeters, P. Newman, R. S. Stolarski, L. Flynn, G. Labow, D. Larko, C. Seftor, C. Wellemeyer, W. D. Komhyr, A. J. Miller, and W. Planet, "Record low global ozone in 1992," *Science, 260*, 523-526, 1993.

Heath, D. F., A. J. Krueger, H. R. Roeder, and B. D. Henderson, "The Solar Backscatter Ultraviolet and Total Ozone Mapping Spectrometer (SBUV/TOMS) for Nimbus G," *Opt. Eng., 14*, 323-331, 1975.

Herman, J. R., R. D. Hudson, and G. Serafino, "Analysis of the eight-year trend in ozone depletion from empirical models of solar backscattered ultraviolet instrument degradation," *J. Geophys. Res.*, 95, 7403-7416, 1990.

Herman, J. R., R. Hudson, R. McPeteres, R. Stolarski, Z. Ahmad, X.-Y. Gu, S. Taylor, and C. Wellemeyer, "A new self-calibration method applied to TOMS/SBUV backscattered ultraviolet data to determine long-term global ozone change," *J. Geophys. Res., 96*, 7531-7545, 1991.

Hudson, R. D., J. R. Herman, and G. Serafino, "On the determination of long-term trends from SBUV ozone data," in *Ozone in the Atmosphere. Proceedings of the Quadrennial Ozone Symposium 1988 and Tropospheric Ozone Workshops*, edited by R. Bojkov and P. Fabian, 189-192. A. Deepak, Hampton, Virginia, 1989.

Klenk, K. F., "Absorption coefficients of ozone for the backscatter UV experiment," *Applied Optics*, 19, Z, 236-242, 1980.

Klenk, K. F., P. K. Bhartia, A. J. Fleig, V. G. Kaveeshwar, R. D. McPeters, and P. M. Smith, "Total ozone determination from the backscattered ultraviolet (BUV) experiment," *J. Appl. Meteorol., 21*, 1672-1684, 1982.

McPeters, R. D., D. F. Heath, and B. M. Schlesinger, "Satellite observation of SO_2 from El Chichón: identification and measurement," *Geophys. Res. Lett., 11*, 1203-1206, 1984.

McPeters, R., and W. D. Komhyr, "Long-term changes in the total ozone mapping spectrometer relative to world primary standard Dobson spectrometer 83," *J. Geophys. Res., 96*, 2987-2993, 1991.

National Aeronautics and Space Administration, "Third and Fourth Year Addendum to the User's Guide for the Total Ozone Mapping Spectrometer (TOMS) Instrument First Year Ozone-T Data Set," Goddard Space Flight Center, Greenbelt, Maryland, 1984.

National Aeronautics and Space Administration, "Nimbus-7 Solar Backscattered Ultraviolet and Total Ozone Mapping Spectrometer (SBUV/TOMS) GRIDTOMS Tape Specifications," Goddard Space Flight Center, Greenbelt, Maryland, 1986.

Paur, R. J., and A. M. Bass, "The ultraviolet cross-sections of ozone: II. Results and temperature dependence," in *Atmospheric Ozone*, edited by C.S. Zerefos and A. Ghazi, 611-616, D. Reidel, Dordrecht, 1985.

Torres, O., Z. Ahmad, and J. R. Herman, "Optical effects of polar stratospheric clouds on the retrieval of TOMS total ozone," *J. Geophys. Res., 97*, 13,015-13,024, 1992.

Watson, R. T., and Ozone Trends Panel, M. J. Prather and Ad Hoc Theory Panel, and M. J. Kuryio and NASA Panel for Data Evaluation, "Present State of Knowledge of the Upper Atmosphere 1988; An Assessment Report," *NASA Reference Publication, 1208*, 33-47, 1988.

Watson, R. T., and Ozone Trends Panel, "Report of the International Ozone Trends Panel 1988," *Rep. 18.* Global Ozone Res. and Monit. Proj., World Meteorol. Organ., Geneva, 1990.

Wellemeyer, C. G., S. L. Taylor, R. R. Singh, and R. D. McPeters, "External comparisons of reprocessed SBUV/TOMS ozone data," *Proceedings of the Quadrennial Ozone Symposium*, 1992.

Wilson, R. C., H. S. Hudson, C. Frohlich, and R. W. Brusa, "Long-term downward trend in solar irradiance," *Science, 234*, 114-117, 1986.

RELATED LITERATURE

Bhartia, P. K., K. F. Klenk, D. Gordon, and A. J. Fleig, "Nimbus-7 total ozone algorithm," Proceedings, 5th Conference on Atmospheric Radiation, American Meteorological Society, Baltimore, Maryland, 1983.

Bhartia, P. K., K. F. Klenk, C. K. Wong, D. Gordon, and A. J. Fleig, "Intercomparison of the Nimbus-7 SBUV/TOMS total ozone data sets with Dobson and M83 results," *J. Geophys. Res., 89,* 5239-5247, 1984.

Bowman, Kenneth P., "Interannual variability of total ozone during the breakdown of the Antarctic circumpolar vortex," *Geophys. Res. Lett., 13,* 1193-1196, 1986.

Bowman, K. P. and A. J. Krueger, "A global climatology of total ozone from the Nimbus-7 Total Ozone Mapping Spectrometer," *J. Geophys. Res., 90,* 7967-7976, 1985.

Bowman, K. P., "Global trends in total ozone," *Science, 239,* 48-50, 1988.

Chandra, S., "The solar and dynamically induced oscillations in the stratosphere," *J. Geophys. Res.*, 91, 2719-2734, 1986.

Chandra, S., "Changes in stratospheric ozone and temperature due to the eruption of Mt. Pinatubo," *Geophys. Res. Lett.*, 20, 33-36, 1993.

Chandra, S., and R. S. Stolarski, "Recent trends in stratospheric total ozone: Implications of dynamical and El Chichón perturbation," *Geophys. Res. Lett., 18,* 2277-2280, 1991.

Dave, J. V., "Multiple scattering in a non-homogeneous, Rayleigh atmosphere," *J. Atmos. Sci., 22,* 273-279, 1965.

Dave, J. V., and Carlton L. Mateer, "A preliminary study on the possibility of estimating total atmospheric ozone from satellite measurements," *J. Atmos. Sci., 24,* 414-427, 1967.

Fraser, R. S., and Z. Ahmad, "The effect of surface reflection and clouds on the estimation of total ozone from satellite measurements." Fourth NASA Weather and Climate Program Science Review, *NASA Conf. Publ. 2076,* 247-252, National Aeronautics and Space Administration, Washington, DC, [NTIS N7920633], 1978.

Fleig, Albert J., R. D. McPeters, P. K. Bhartia, Barry M. Schlesinger, Richard P. Cebula, K. F. Klenk, Steven L. Taylor, and D. F. Heath, "Nimbus-7 Solar Backscatter Ultraviolet (SBUV) ozone products user's guide," *NASA Reference Publication, 1234,* National Aeronautics and Space Administration, Washington, DC, 1990.

Heath, D. F., and H. Park, "The Solar Backscatter Ultraviolet (SBUV) and Total Ozone Mapping Spectrometer (TOMS) experiment," in *The Nimbus-7 Users' Guide*, edited by C. R. Madrid, 175-211, NASA Goddard Space Flight Center, Greenbelt, Maryland, 1978.

Heath, D. F., "Non-Seasonal Changes in Total Column Ozone From Satellite Observations," 1970-1986, *Nature, 332*, 219-227, 1988.

Heath, D. F., "Changes in the vertical distribution of stratospheric ozone and the associated global scale changes in total ozone from observations with the Nimbus-7 SBUV instrument; 1978-1986," in *Proceedings of the International Ozone Symposium*, edited by R. Bojkov and P. Fabian, p. 810, A. Deepak, Hampton, Virginia, 1990.

Herman, J. R., R. McPeters, R. Stolarski, D. Larko, and R. Hudson, "Global average ozone change from November 1978 to May 1990," *J. Geophys. Res.*, 96, 17279-17305, 1991.

Herman, J. R., R. McPeters, and D. Larko, "Ozone depletion at northern and southern latitudes derived from January 1979 to December 1991 TOMS data," accepted for publication, *J. Geophys. Res., 98*, 1993.

Herman, J. R. and D. Larko, "Global ozone change as a function of latitude and longitude: January 1979 to December 1991," submitted to *J. Geophys. Res.*, 1993.

Herman, J. R., D. Larko, "Nimbus–7/TOMS-November 1, 1978 to May 6, 1993: Low ozone amounts during 1992–1993," submitted to *J. Geophys. Res.*, 1993.

Klenk, K. F., P. K. Bhartia, E. Hilsenrath, and A. J. Fleig, "Standard ozone profiles from balloon and satellite data sets," *J. Climate Appl. Meteorol., 22*, 2012-2022, 1983.

Komhyr, W. D., R. D. Grass, and R. K. Leonard, "Total ozone, ozone vertical distributions, and stratospheric temperatures at South Pole, Antarctica, in 1986 and 1987," *J. Geophys. Res., 94*, 11,429-11,436, 1989.

Krueger, A. J., M. R. Schoeberl, and R. S. Stolarski, "TOMS observations of total ozone in the 1986 Antarctic spring," *Geophys. Res. Lett., 14*, 527-530, 1987.

Larko, David E., Louis W. Uccellini, and Arlin J. Krueger, "Atlas of TOMS ozone data collected during the Genesis of Atlantic Lows Experiment (GALE)" *NASA-TM-87809,* 99 pp., 1986.

Lienesch, J. H. and P. K. K. Pandey, "The use of TOMS data in evaluating and improving the total ozone from TOVS measurements," *Rep. NOAA-TR-NESDIS-23, Issue 22*, 3814-3828, 1985.

Logan, J. A., "Tropospheric ozone: Seasonal behavior, trends, and anthropogenic influence," *J. Geophys. Res., 90,* 10,463-10,482, 1985.

Pommereau, J. P., F. Goutail, H. LeTexier, and T. S. Jorgensen, "Stratospheric ozone and nitrogen dioxide monitoring at southern and northern polar latitudes," in *Our Changing Atmosphere, Proceedings of the 28th Liege International Astrophysical Colloquium,* edited by P. Crutzen. J.-C. Gerard, and R. Zander, University de Liege, Liege, Belgium, 1989.

Schoeberl, Mark R., Arlin J. Krueger, and Paul A. Newman, "The morphology of Antarctic total ozone as seen by TOMS -- Total Ozone Mapping Spectrometer," *Geophys. Res. Lett., 13,* 1217-1220, 1986.

Schoeberl, M. R., P. K. Bhartia, E. Hilsenrath, and O. Torres, "Tropical ozone loss following the eruption of Mt. Pinatubo," *Geophys. Res. Lett., 20,* 29-32, 1993.

Solomon, S., "Antarctic ozone: Progress towards a quantitative understanding," *Nature, 347,* 347-354, 1990.

Stolarski, R. S., A. J. Krueger, M. R. Schoeberl, R. D. McPeters, P. A. Newman, and J. C. Alpert, "Nimbus-7 satellite measurements of the springtime Antarctic ozone decrease," *Nature, 322,* 808-811, 1986.

Stolarski, R. S., "Observations of global stratospheric ozone change," *Ber. Bunsen Ges. Phys. Chem.,* 96, 258-263, 1992.

Stolarski, R. S., P. Bloomfield, R. D. McPeters, and J. R. Herman, "Total ozone trends deduced from Nimbus-7 TOMS data," *Geophys. Res. Lett., 18,* 1015-1018, 1991.

Stolarski, R. S., L. Bishop, R. Bojkov, M. L. Chanin, V. Fioletev, V. Kircchoff, J. Zawodny, and C. Zerefos, "Ozone and temperature trends," in Scientific Assessment of Ozone Depletion; 1991, *WMO Rep. 25,* 2.1-2.30, World Meteorol. Organ., Geneva, 1992.

Stolarski, R. S., R. Bojkov, L. Bishop, C. Zerefos, J. Staehelin, and J. Zawodny, "Measured trends in stratospheric ozone," *Science 256,* 342-349, 1992.

Vigroux, Ernest, "Contribution a l etude experimental de l'absorption de l'ozone," *Ann. Phys., ser. 12, 8,* 709-762, 1953.

Vigroux, E., "Determination des coefficients moyen d'absorption de l'ozone en vue des observations concernant l'ozone atmospherique a l'aide du spectrometre Dobson," *Ann. Phys., ser. 14, 2,* 209-215, 1967.

Wellemeyer, C., A. J. Fleig, and P. K. Bhartia, "Internal comparisons of SBUV and TOMS total ozone measurements," in *Proceedings of the International Ozone Symposium*, edited by R. Bojkov and P. Fabian, 193-197, A. Deepak, Hampton, Virginia, 1989.

LIST OF ACRONYMS, INITIALS, AND ABBREVIATIONS

a.u.	astronomical units
bpi	bits per inch
BUV	Backscatter Ultraviolet
EBCDIC	Extended Binary Coded Decimal Interchange Code
FB	Fixed Block
FOV	Field-of-View
GMT	Greenwich Mean Time
GRIDTOMS	Gridded TOMS Tape
IFOV	Instantaneous Field-of-View
IPD	Information Processing Division
LSB	Least Significant Bit
MSB	Most Significant Bit
NIST	National Institute of Standards and Technology
NET	Nimbus Experiment Team
NMC	National Meteorological Center
NOAA	National Oceanic and Atmospheric Administration
NOPS	Nimbus Ozone Processing System
NSSDC	National Space Science Data Center
OPT	Ozone Processing Team
PDF	Product Definition File
PMT	Photomultiplier Tube
RUT	Raw Units Tape

SACC	Science and Applications Computing Center
SBUV	Solar Backscatter Ultraviolet
SOI	SO_2 Index
SPAN	Space Physics Analysis Network
TDF	Trailer Documentation File
THIR	Temperature-Humidity Infrared Radiometer
TOMS	Total Ozone Mapping Spectrometer
UV	Ultraviolet

APPENDIX A DATA QUALITY FLAG

The data quality flag describes the quality of the retrieved total ozone values. The flag value for the first sample appears in bytes 1 and 2 of word 12 of the data record of the HDTOMS tape, and those for subsequent samples are in the first two bytes of every seventh word thereafter. The flag value describes the quality of Best ozone for the same sample. The data quality flag is a two-digit integer. The units digit is an indicator of the quality of the total ozone values. The tens digit signifies whether the measurement was made on the ascending or descending part of the orbit. Table A.1 summarizes the significance of each flag.

Total ozone data quality degrades as the optical path of the ultraviolet radiation through the atmosphere increases. For the purposes of setting data flag indicators, optical path is defined to be the product of air mass and total column ozone, in units of atm-cm. In the TOMS viewing geometry, the range of solar zenith angles corresponding to a given path designation depends upon the zenith angle of the satellite at the field-of-view, which ranges from 0° for a nadir measurement to 63° at the beginning or end of a scan. The satellite zenith angle at the extreme off-nadir FOV is larger than the maximum 51° angle between the nadir and the direction of the scan from the satellite because of the curvature of the Earth. For example, for a typical 350 matm-cm column ozone amount, low path (flag value 0) would represent all nadir measurements with solar zenith angles less than 72° and all extreme off-nadir measurements, with solar zenith angles less than 61°; high path (1) would include nadir measurements with zenith solar angles in the 72°-84° range, and extreme off-nadir measurements with zenith solar angles in the 61°-83° range; and very high path (2) would extend up to 88° for all measurements. Data are not processed for solar zenith angles greater than 88°. A flag value of 3 denotes that contamination by SO_2 is likely. When there is a significant quantity of SO_2 in the atmosphere, it absorbs the backscattered radiation over a region of the spectrum that includes many of the wavelengths used in total ozone retrieval. The ozone value retrieved by the algorithm will thus be incorrect. The SO_2 index, a function of the measured radiances designed to be sensitive to SO_2 but relatively insensitive to ozone, is used to identify scans so affected. A value of 4 for the units digit indicates that one or more of the differences among the three total ozone values derived independently from the three wavelength pairs is outside a selected tolerance. Flag 4 rarely occurs at low solar zenith angles. However, at large solar zenith angles, a user may wish to accept total ozone values with a data quality flag of 4 if noisy data are preferable to no data at all. Such situations normally occur near the winter solstice. When the latitude of the terminator approaches 67°, there may be no total ozone measurements close to the terminator with flags less than 4.

Table A.1. HDTOMS Data Quality Flags

Units Digit	
0	Low path (air mass x total ozone ú 1.5 atm-cm).
1	High path (1.5 atm-cm < air mass x total ozone < 3.5 atm-cm).
2	Very high path (3.5 atm-cm < air mass x total ozone).
3	SO_2 contamination.
4	Inconsistent A, B, C pair values.
7	Reflectivities at 360 nm and 380 nm inconsistent.
8	Implausible reflectivity.
9	Implausible ozone value.
Tens Digit	
0x	Ascending part of orbit (80°S to 80°N).
1x	Descending part of orbit.

Flag values of 7 and 8 indicate that the reflectivity is suspect: the value of 7 is used when the reflectivities at the two TOMS wavelengths are inconsistent; a value of 8 denotes a physically implausible value for the reflectivity. These conditions will, in general, arise because of an instrument malfunction, data transmission problem, or tape error associated with a particular measurement. Data with flag values of 7 or 8 should normally not be used. Flag values of 5 or 9, denoting physically unlikely ozone values, will in most cases, arise from the same types of problems that lead to flag values of 7 or 8. However, unusual values of ozone associated with rare physical conditions may also carry a quality flag of 5 or 9.

Finally, the tens digit distinguishes TOMS data taken during the ascending part of the Nimbus-7 orbit (as the satellite moves from 80°S to 80°N) from data taken during the descending part (80°N to 80°S). During most of the descending part of the orbit, the subsatellite point is in darkness, and no ozone measurements are possible. However, at high latitudes near the summer pole, in the regions of midnight Sun, data will be obtained twice at the same latitude: once from the normal midday ascending measurement, and once from the nightside descending orbit measurement. These data from the descending part of the orbit will have a larger solar zenith angle and path length than those for the ascending part of the orbit at the same latitude; they will,

in general, be less accurate. We recommend that data with a flag of 1 in the tens place, for the descending part of the orbit, normally not be used for analysis.

Additional detail about the validity checks and the conditions leading to the flagging of data appear in Section 6.5.

To summarize, the best compromise between coverage and data quality is obtained by accepting flags 0, 1, and 2 .

APPENDIX B
FORTRAN PROGRAMS TO READ HDTOMS AND GRIDTOMS TAPES

FORTRAN routines and sample output are provided for HDTOMS and GRIDTOMS respectively.

```
CCCCCCCCCCCCCCCCCCCCCCCCCCCCCCCCCCCCCCCCCCCCCCCCCCCCCCCCCCCCCCCCCCCCCCC
C
C  SUBROUTINE TO UNPACK AND DISPLAY THE HDTOMS DATA RECORD
C    ACCEPTS INTEGER*2 I2HDT(2,252) ARRAY AS INPUT
C
CCCCCCCCCCCCCCCCCCCCCCCCCCCCCCCCCCCCCCCCCCCCCCCCCCCCCCCCCCCCCCCCCCCCCCC
C
      SUBROUTINE HDTDMP(I2HDT,RLAT,RLON,SZA,THRPRE,REFL,
     1  RFPRES,BESTOZ,APROZ,BPROZ,TOTLOZ,
     2  TERROZ,SURPRE,CPROZ,SOI,ISNOW,IQCFLG,
     3  RN1VAL,RN2VAL,RN3VAL,RN4VAL,RN5VAL,
     4  RN6VAL,IDAY,ICHSYF,ISEQ,PHI,IGMT,ORBIT,FIRST,IYEAR)
C
      DIMENSION RLAT(35),RLON(35),SZA(35),THRPRE(35),REFL(35),
     1  RFPRES(35),BESTOZ(35),APROZ(35),BPROZ(35),TOTLOZ(35),
     2  TERROZ(35),SURPRE(35),CPROZ(35),SOI(35),ISNOW(35),IQCFLG(35),
     3  RN1VAL(35),RN2VAL(35),RN3VAL(35),RN4VAL(35),RN5VAL(35),
     4  RN6VAL(35)
      INTEGER*2 I2HDT(2,252),IDAY,ICHSYF,ISEQ,IPHI,I2HOLD
C
      IDAY = I2HDT(2,2)
      ISEQ = I2HDT(1,2)
      IPHI = I2HDT(2,5)
      ICHSYF = I2HDT(1,5)
      PHI = IPHI / 100.0
C
C  UNPACK EACH OF THE 35 SAMPLES
C
      DO 100 ISAMPL = 1,35
        ISAMP = ((ISAMPL - 1) * 7) + 5
        RLAT(ISAMPL) = I2HDT(1,ISAMP + 1) / 100.0
        RLON(ISAMPL) = I2HDT(2,ISAMP + 1) / 100.0
        IF(I2HDT(1,ISAMP+2).GE.0) THEN
          SZA(ISAMPL) = I2HDT(1,ISAMP + 2) / 100.0
        ELSE
          SZA(ISAMPL) = I2HDT(1,ISAMP + 2)
        END IF
        REFL(ISAMPL) = I2HDT(1,ISAMP + 3)
        IHOLD = I2HDT(2,ISAMP + 3)
        IHD = MOD(IHOLD,10)
        RFPRES(ISAMPL) = (IHD+1)/10.0
        BESTOZ(ISAMPL) = I2HDT(1,ISAMP + 4)
C
        I2HOLD = I2HDT(2,ISAMP + 4)
        CALL BYTE(I2HOLD,MSB,LSB)
        XMSB = MSB
        XLSB = LSB
        IF(XMSB.GE.0.0) THEN
          APROZ(ISAMPL) = XMSB * 3.0
        ELSE
          APROZ(ISAMPL) = XMSB
        END IF
        IF(XLSB.GE.0.0) THEN
          BPROZ(ISAMPL) = XLSB  * 3.0
        ELSE
          BPROZ(ISAMPL) = XLSB
```

```
        END IF
C
        I2HOLD = I2HDT(1,ISAMP + 5)
        CALL BYTE(I2HOLD,MSB,LSB)
        XLSB = LSB
        TERROZ(ISAMPL) = XLSB
        IF(XLSB.EQ.-77.0) TERROZ(ISAMPL) = 0.0
        IHOLD = I2HDT(2,ISAMP + 5)
        IHD = MOD(IHOLD,10)
        SURPRE(ISAMPL) = (IHD+1)/10.0
C
        I2HOLD = I2HDT(1,ISAMP + 6)
        CALL BYTE(I2HOLD,MSB,LSB)
        XMSB = MSB
        XLSB = LSB
        IF(XMSB.GE.0.0) THEN
          CPROZ(ISAMPL) = XMSB * 3.0
        ELSE
          CPROZ(ISAMPL) = XMSB
        END IF
C
        IF(XLSB.GT.0.0) THEN
          SOI(ISAMPL) = XLSB - 100.0
        ELSE
          SOI(ISAMPL) = XLSB
        END IF
C
        IHOLD = I2HDT(2,ISAMP + 6)
        ISNOW(ISAMPL) = MOD(IHOLD,10)
        IQCFLG(ISAMPL) = I2HDT(1,ISAMP + 7)
C
        I2HOLD = I2HDT(2,ISAMP + 7)
        CALL BYTE(I2HOLD,MSB,LSB)
        XMSB = MSB
        XLSB = LSB
        RN4VAL(ISAMPL) = (I2HDT(2,ISAMP+6) / 10) / 10.0
        RN3VAL(ISAMPL) = (I2HDT(2,ISAMP+5) / 10) / 10.0
        RN2VAL(ISAMPL) = (I2HDT(2,ISAMP+3) / 10) / 10.0 + RN4VAL(ISAMPL
        RN1VAL(ISAMPL) = (I2HDT(2,ISAMP+2) / 10) / 10.0 + RN3VAL(ISAMPL
        RN5VAL(ISAMPL) = (XMSB - 100) / 10.0 + RN4VAL(ISAMPL)
        RN6VAL(ISAMPL) = (XLSB - 100) / 10.0 + RN5VAL(ISAMPL)
  100 CONTINUE
C
C  PRINTOUT DATA RECORD
C
      WRITE(6,2000) ISEQ,IDAY,IGMT,ICHSYF,PHI,ORBIT
      WRITE(6,2100)
C
      DO 200 IS = 1,35
        WRITE(6,2200) IS,RLAT(IS),RLON(IS),SZA(IS),
     1  REFL(IS),RFPRES(IS),BESTOZ(IS),APROZ(IS),BPROZ(IS),
     2  TERROZ(IS),SURPRE(IS),CPROZ(IS),SOI(IS),ISNOW(IS),IQCFLG(IS),
     3  RN1VAL(IS),RN2VAL(IS),RN3VAL(IS),RN4VAL(IS),RN5VAL(IS),
     4  RN6VAL(IS)
  200 CONTINUE
C
      RETURN
C
C  FORMATS
C
```

HDTOMS

```
 2000 FORMAT(/2X,' SEQ NO.-',I5,' DAY-',I5,' GMT-',I5,' CHOP NON-SYNC-'
     1  I5,' PHI ANGLE-',F6.1,' ORBIT-',F6.0)
 2100 FORMAT(/23X,'THIR',8X,'REFL BEST  APAIR BPAIR  THIR TERAN  ',
     1  'SURF CPAIR',12X,'QUAL N-VAL N-VAL N-VAL N-VAL N-VAL N-VAL',/,
     2  2X,'IS LAT.  LON.   SZA  PRES  REFL  PRES OZONE OZONE OZONE',
     3  ' OZONE OMEGA  PRES OZONE   SOI SNOW FLAG  3125  3175  3312',
     4  '  3398  3600  3800')
 2200 FORMAT(1X,I2,3F6.1,6X,5F6.1,6X,4F6.1,2I4,2X,6F6.1)
      END
CCCCCCCCCCCCCCCCCCCCCCCCCCCCCCCCCCCCCCCCCCCCCCCCCCCCCCCCCCCCCCCCCCCCCCC
C
C  SUBROUTINE TO SEPERATE UPPER AND LOWER BYTES OF I*2 WORDS
C    AND RETURN AS POSITIVE I*4 QUANTITIES
C    SINGLE BYTE HDTOMS VALUES OF 0 INDICATE MISSING DATA
C
CCCCCCCCCCCCCCCCCCCCCCCCCCCCCCCCCCCCCCCCCCCCCCCCCCCCCCCCCCCCCCCCCCCCCCC
      SUBROUTINE BYTE(I2WD,MSB,LSB)
C
      INTEGER*2 I2WD,I2MAP(2)
      EQUIVALENCE (I2MAP(1),I4DATA)
C
      I2MAP(2) = I2WD
      MSB = ISHFT(I4DATA,-8)
      LSB = I4DATA - ISHFT(MSB,8)
C
      IF (MSB .LE. 0) MSB = -77
      IF (LSB .LE. 0) LSB = -77
C
      RETURN
      END
```

SEQ NO.- 223 DAY- 79 GMT-22295 CHOP NON-SYNC- 0 PHI ANGLE- -59.0 ORBIT- 2032.

IS	LAT.	LON.	SZA	THIR PRES	REFL PRES	REFL BEST OZONE	APAIR OZONE	BPAIR OZONE	THIR OZONE	TERAN OMEGA	SURF PRES	CPAIR OZONE	SOI	SNOW	QUAL FLAG	N-VAL 3125	N-VAL 3175	N-VAL 3312	N-VAL 3398	N-VAL 3600	N-VAL 3800
1	13.8	95.3	15.5		8.0	1.0	275.0	276.0	270.0	0.0	1.0	249.0	2.0	0	0	147.2	121.6	99.2	97.8	103.5	109.0
2	13.6	93.6	14.8		7.0	1.0	274.0	273.0	270.0	0.0	1.0	-77.0	-1.0	0	0	143.6	120.3	100.5	99.4	105.7	111.7
3	13.5	92.3	14.3		7.0	1.0	274.0	273.0	273.0	0.0	1.0	-77.0	3.0	0	0	141.1	119.6	101.1	100.5	107.2	113.0
4	13.4	91.2	13.9		7.0	1.0	274.0	273.0	273.0	0.0	1.0	-77.0	5.0	0	0	139.3	119.0	101.8	101.3	108.0	114.3
5	13.3	90.2	13.7		8.0	1.0	275.0	276.0	273.0	0.0	1.0	-77.0	2.0	0	0	138.1	118.2	102.1	101.7	108.4	114.5
6	13.2	89.4	13.6		7.0	1.0	275.0	276.0	273.0	0.0	1.0	-77.0	3.0	0	0	137.1	118.0	102.5	102.4	109.1	115.2
7	13.1	88.6	13.5		7.0	1.0	273.0	273.0	270.0	0.0	1.0	-77.0	1.0	0	0	136.4	118.0	103.5	103.5	110.5	116.9
8	13.0	87.9	13.4		6.0	1.0	272.0	273.0	270.0	0.0	1.0	-77.0	6.0	0	0	135.5	117.8	103.7	104.0	111.0	117.5
9	12.9	87.3	13.4		6.0	1.0	270.0	270.0	267.0	0.0	1.0	-77.0	1.0	0	0	134.5	117.3	103.9	104.2	111.4	117.6
10	12.8	86.7	13.4		6.0	1.0	268.0	267.0	267.0	0.0	1.0	-77.0	8.0	0	0	133.6	117.0	103.9	104.4	111.4	117.6
11	12.8	86.1	13.5		7.0	1.0	269.0	270.0	267.0	0.0	1.0	-77.0	11.0	0	0	133.0	116.6	103.5	104.0	111.0	116.7
12	12.7	85.6	13.5		8.0	1.0	268.0	267.0	261.0	0.0	1.0	-77.0	4.0	0	0	132.3	115.9	103.2	103.7	110.2	115.9
13	12.7	85.1	13.6		9.0	1.0	269.0	267.0	267.0	0.0	1.0	-77.0	9.0	0	0	131.7	115.7	102.8	103.1	109.4	114.6
14	12.6	84.6	13.7		10.0	1.0	268.0	267.0	264.0	0.0	1.0	-77.0	0.0	0	0	131.1	114.8	102.1	102.2	107.9	112.6
15	12.5	84.1	13.8		11.0	1.0	269.0	267.0	267.0	0.0	1.0	-77.0	2.0	0	0	130.4	114.3	101.4	101.3	106.8	111.1
16	12.5	83.7	13.9		14.0	1.0	266.0	267.0	264.0	0.0	1.0	-77.0	5.0	0	0	128.4	112.3	99.2	99.0	103.9	107.8
17	12.4	83.2	14.0		15.0	1.0	265.0	264.0	267.0	0.0	1.0	-77.0	1.0	0	0	127.8	111.9	98.7	98.2	102.9	106.4
18	12.3	82.7	14.2		12.0	1.0	265.0	264.0	267.0	0.0	1.0	-77.0	1.0	0	0	129.2	113.5	100.7	100.5	105.6	109.5
19	12.3	82.3	14.3		11.0	1.0	266.0	264.0	267.0	0.0	1.0	-77.0	-5.0	0	0	129.6	113.7	101.1	100.9	106.6	111.1
20	12.2	81.8	14.5		10.0	1.0	265.0	264.0	264.0	0.0	1.0	-77.0	4.0	0	0	129.8	114.0	101.6	101.7	107.4	112.1
21	12.2	81.3	14.7		9.0	1.0	266.0	267.0	264.0	0.0	1.0	-77.0	1.0	0	0	130.0	114.0	101.6	101.7	108.0	113.2
22	12.1	80.9	14.9		9.0	1.0	266.0	267.0	264.0	0.0	1.0	-77.0	8.0	0	0	129.8	113.8	101.1	101.5	107.6	113.2
23	12.0	80.4	15.1		7.0	1.0	266.0	267.0	261.0	0.0	1.0	-77.0	6.0	0	0	130.8	114.7	102.3	102.8	109.6	115.8
24	11.9	79.9	15.3		8.0	1.0	269.0	267.0	270.0	0.0	1.0	-77.0	16.0	0	0	130.6	114.5	101.1	101.5	108.0	113.9
25	11.9	79.3	15.6		9.0	1.0	269.0	270.0	267.0	1.0	1.0	-77.0	5.0	0	0	131.7	114.9	101.6	101.7	108.4	113.8
26	11.8	78.8	15.9		4.0	1.0	268.0	267.0	267.0	1.0	1.0	-77.0	-7.0	0	0	134.5	117.5	104.9	105.1	112.8	119.6
27	11.7	78.2	16.2		5.0	0.9	267.0	267.0	264.0	2.0	0.9	-77.0	-5.0	0	0	135.0	117.6	104.4	104.7	111.7	118.5
28	11.6	77.5	16.5		4.0	0.9	267.0	267.0	261.0	2.0	0.9	-77.0	2.0	0	0	135.9	118.3	104.7	105.1	112.6	119.7
29	11.5	76.8	16.9		3.0	0.9	268.0	267.0	270.0	2.0	0.9	-77.0	5.0	0	0	137.6	120.1	105.9	106.1	113.9	120.9
30	11.3	76.1	17.4		12.0	1.0	270.0	270.0	264.0	1.0	1.0	-77.0	7.0	0	0	134.1	114.8	98.5	98.2	103.5	108.2
31	11.2	75.2	17.9		8.0	1.0	269.0	267.0	267.0	1.0	1.0	-77.0	4.0	0	0	135.7	116.1	99.8	99.4	105.9	111.7
32	11.0	74.3	18.6		8.0	1.0	271.0	270.0	270.0	0.0	1.0	-77.0	8.0	0	0	137.1	116.6	98.9	98.4	104.5	110.2
33	10.8	73.1	19.4		9.0	1.0	270.0	270.0	267.0	0.0	1.0	-77.0	-3.0	0	0	138.8	116.8	98.3	97.2	103.1	108.6
34	10.6	71.8	20.3		9.0	1.0	268.0	267.0	267.0	0.0	1.0	264.0	0.0	0	0	140.9	117.6	97.3	95.9	101.5	106.7
35	10.3	70.1	21.6		11.0	1.0	271.0	270.0	267.0	0.0	1.0	267.0	-3.0	0	0	145.0	119.0	96.0	94.0	98.9	103.7

GRIDTOMS

```
CCCCCCCCCCCCCCCCCCCCCCCCCCCCCCCCCCCCCCCCCCCCCCCCCCCCCCCCCCCCCCCCCCCCCC
C
C  PROGRAM GRIDTDMP:
C
C  PROGRAM TO READ GRIDT TAPE AND LOAD PARAMETERS IN MAP ARRAY
C   MAP(288,180,3) IS IMAGE STYLE WITH:
C     1-288 FROM 180 W - 180 E LONGITUDE
C     1-180 FROM 90 N - 90 S LATITUDE
C     1-3 FOR PARAMETERS; GMT (HOURS * 1000), OZONE (DU), REFL (%)
C
CCCCCCCCCCCCCCCCCCCCCCCCCCCCCCCCCCCCCCCCCCCCCCCCCCCCCCCCCCCCCCCCCCCCCC
C
      INTEGER*2 I2REC(882),I2DAT(3,288),I2SEQ
      CHARACTER*8 INTAPE
      LOGICAL*4 FRSTRC
      EQUIVALENCE (I2REC(11),I2DAT(1,1)),(I2REC(3),I2SEQ)
C
      COMMON/DATA/MAP(288,180,3)
C
      READ(5,1000,END=500) INTAPE,INDAY
      WRITE(6,1000) INTAPE,INDAY
C
      CALL MOUNT(1,20,INTAPE,2)
      NFILE = 1
C
  100 CONTINUE
      NFILE = NFILE + 1
      CALL POSN(1,20,NFILE)
      FRSTRC = .TRUE.
C
      DO 200 IREC=1,180
C
      CALL FREAD(I2REC,20,LEN,*300,*400)
C
      IF(FRSTRC) THEN
        IF(I2SEQ.EQ.-1) GO TO 500
        FRSTRC = .FALSE.
        IDAY = I2REC(10)
        IYEAR = I2REC(9)
        IF(IDAY.NE.INDAY) GO TO 100
      ENDIF
C
      CALL LODMAP(IREC,I2DAT)
C
  200 CONTINUE
C
C  PRINTOUT DESIRED PORTION OF MAP ARRAY
C
      WRITE(6,2000) IDAY,IYEAR,((MAP(I,J,2),I=240,264),J=101,131)
      GO TO 500
C
C  I/O ERROR EXITS
C
  300 CONTINUE
      WRITE(6,3000) INTAPE,NFILE,IREC
      GO TO 500
C
C  UNEXPECTED END OF FILE
C
```

GRIDTOMS

```
  400 CONTINUE
      WRITE(6,3100) INTAPE,NFILE
C
  500 CONTINUE
      STOP
C
C  FORMATS
C
 1000 FORMAT(1X,'INTAPE=',A8,'INDAY=',I4)
 2000 FORMAT(/,1X,'OZONE MAP OVER AUSTRALIA FOR DAY',I5,',',I5,//,
     1    31(1X,25I4,/))
 3000 FORMAT(//1X,'*** I/O ERROR ENCOUNTERED AT ',A8,2I4,' ***',//)
 3100 FORMAT(//1X,'*** UNEXPECTED END OF FILE ON ',A8,I4,' ***',//)
      END
      SUBROUTINE LODMAP(IREC,I2DAT)
C
      DIMENSION NCELLS(180)
      INTEGER*2 I2DAT(3,288)
C
      COMMON/DATA/MAP(288,180,3)
C
      DATA NCELLS/20*72,20*144,100*288,20*144,20*72/
C
      DO 200 ICELL=1,NCELLS(IREC)
        DO 100 IPARAM=1,3
          INDEX = IPARAM
          MAP(ICELL,181-IREC,IPARAM) = I2DAT(INDEX,ICELL)
  100   CONTINUE
  200 CONTINUE
C
      RETURN
C
      END
```

```
INTAPE=GRID6C  INDAY=  94

OZONE MAP OVER AUSTRALIA FOR DAY   94, 1990

 281 279 281 281 280 281 281 279 279 279 279 278 278 274 275 280 279 278 270 268 268 276 271 269 268
 282 280 281 282 281 280 281 279 279 278 276 275 273 271 275 277 279 279 275 274-777 277 272 270 267
 280-777 277 279 279 278 278 278 276 276 276 273 275 274 275 277 279 278 273 273 271 275 274 271 270
 279-777 277 276 276 275 274 275 275 275 275 276 274 274 276 278 279 277 277 275 272 273-777 273 271
-777 276 274 274 273 274 274 273 274 275 275 274 273 275 276 276 279 277 277 276 274 272 270 271 270
 272 275 275 273 273 273 270 271 272 273 273 273 273 272 274 275 276 276 275 273 272 270 272 269 269
 273 275 273 271 273 273 269 270 271 272 272 272 272 270 271 273 273 273 272 272-777 273 273 271 269
 274 273 271 272 272 271 270 270 271 272 270 270 270 270 269 270 271 270 272 272 273 273 274 271 271
 272 273 272 271 271 271 271 271 271 269 269 269 269 268 269 268 270 270 270 271 272 274 274 273 271
 270 271 271 269 270 270 269 270 271 268 269 268 269 269 270 267 269 269 269 269 272 273 275 273 272
 271 272 271 271 270 269 271 269 269 270 269 269 270 270 270 271 270 273 271 269 271-777 272 273 275
 270 270 271 271 271 270 271 272 272 270 269 268 269 270 269 272 274 275 274 275 275 272 274 272 281
 271 271 273 271 272 272 271 273 272 271 270 269 271 270 271 271 274 274 275 275 275 274 275 283 283
 272-777 272 272 271 272 273 272 273 272 270 270 271 271 271 272 271 273 273 276 278 277 280 284 292
 276 274 273 274 273 273 274 274 273 274 273 271 273 271 271 272 271 272 273 273 278 282 280 287 293
 278 277 275 274 278 276 275 276 277 274 274 274 275 273 273 273 272 276 273 274 274 282 288 285 294
 279 281 278 280 279 277 278 276 278 276 276 274 275 276 275 275 276 275 274 278 278 286 291 290 292
 281 282 282 278 279 280 279 278 281 278 277 275 275 277 277 279 278 277 278 279 280 282 291 292 286
 280 285 284 282 282 282 282 281 281 281 281 276 275 276 279 281 279 280 280 291 299 296 293 290 284
 286 286 286 285 288 285 282 284 282 282 281 279 277 277 278 280 279 280 281 284 295 292 291 277 284
 285 287 284 288 291 288 285 285 288 285 282 281 280 280 281 282 281 280 282 284 287 286 290 282 283
 286 288 288 287 292-777 292 290 289 290 287 286 281 280 283 282 280 281 283 285 290 282 288 280 282
 293 290 291 290 291 294 291 292 291 291 288 287 284 283 283 281 279 280 282 281 288 286 280 281 285
 293 295 298 298 293 293 291 290 288 289 286 285 281 280 280 281 278 278 281 281 285 286 281 283 285
 295 294 298 301 296 290 285 286 284 285 281 281 277 277 279 279 280 280 281 281 282 285 286 282 284
 299 298 299 301 298 298 292 287 282 282 280 279 277 276 278 278 277 278 280 280 280 282 285 285 292
 304 306 303 312 300 297 293 285 282 280 280 280 278 277 278 278 278 277 277 277 278 278 279 281 287
 311 311 309 308 302 298 296 280 279 279 280 279 279 279 277 279 278 277 275 276 274 274 277 277 278
 307 306 307 299 300 297 293 295 283 276 280 281 279 280 277 278 276 275 275 275 276 276 276 277 280
 307 307 302 302 296 303 292 294 286 275 277 280 281 281 280 278 276 274 273 276 278 276 276 278 281
 309 316 303 300 302 303 299 296 288 275 274 276 279 279 275 277 274 275 274 274 278 279 277 278 280
```

APPENDIX C

TOMS Standard Temperature Profiles (°Kelvin)

UMKEHR Layer	Central PRESSURE (MBAR)	Latitude Band Low	Mid	High
10	0.75	271	268	261
9	1.50	270	265	256
8	3.00	261	254	243
7	6.00	248	240	235
6	12.00	234	229	227
5	24.00	222	222	221
4	48.00	210	217	222
3	95.00	201	214	222
2	190.00	214	216	221
1	380.00	251	239	228
0	760.00	283	273	260

Temperature Profiles Used at Low Ozone Conditions

UMKEHR Layer	Central Pressure (MBAR)	Ozone Amount (D.U.) 125	175
10	0.75	272	272
9	1.50	272	272
8	3.00	260	266
7	6.00	240	254
6	12.00	220	238
5	24.00	210	225
4	48.00	193	206
3	95.00	191	196
2	190.00	196	196
1	380.00	218	218
0	760.00	237	237

APPENDIX D

Standard Ozone Profiles
(matm-cm)

High Latitude (75°)

	Total Ozone (D.U.)				
Layer	125	175	225	275	325
0,1	16.5	17.5	18.0	26.0	29.0
2	18.3	22.8	24.6	30.5	40.8
3	7.6	21.0	41.7	62.9	78.6
4	8.2	24.9	46.0	59.2	71.2
5	28.6	35.3	38.0	38.5	45.7
6	22.0	26.8	28.8	28.8	28.8
7	12.4	15.0	15.4	15.4	17.2
8	7.7	8.0	8.3	8.9	8.9
9	2.5	2.5	2.9	3.4	3.4
10	1.2	1.2	1.3	1.4	1.4

High Latitude (75°) (Continued)

	Total Ozone (D.U.)				
Layer	375	425	475	525	575
0,1	33.0	38.0	45.0	54.0	58.1
2	53.2	68.7	85.0	104.1	114.0
3	89.8	100.9	114.1	128.1	134.8
4	82.2	91.2	99.0	105.0	114.0
5	51.9	56.9	59.8	60.2	75.8
6	32.5	35.6	37.5	38.2	40.2
7	18.7	20.0	20.9	21.7	21.7
8	8.9	8.9	8.9	8.9	10.7
9	3.4	3.4	3.4	3.4	4.1
10	1.4	1.4	1.4	1.4	1.6

Mid Latitude (45°)

Layer	Total Ozone (D.U.) 125	175	225	275	325
0,1	16.5	17.5	27.0	28.0	30.0
2	18.3	22.8	12.0	15.0	26.0
3	7.6	21.0	14.0	29.0	45.0
4	8.2	24.9	40.0	58.0	74.7
5	28.6	35.3	52.1	63.7	66.9
6	22.0	26.8	39.2	40.6	41.7
7	12.4	15.0	24.5	24.5	24.5
8	7.7	8.0	11.1	11.1	11.1
9	2.5	2.5	3.7	3.7	3.7
10	1.2	1.2	1.4	1.4	1.4

Mid Latitude (45°) (Continued)

Layer	Total Ozone (D.U.) 375	425	475	525	575
0,1	32.0	34.0	38.0	42.0	58.1
2	39.0	54.0	72.0	91.0	114.0
3	64.0	84.0	107.7	131.7	134.8
4	85.7	97.7	101.0	108.0	114.0
5	71.1	71.7	72.6	68.8	75.8
6	42.5	42.9	43.0	42.8	40.2
7	24.5	24.5	24.5	24.5	21.7
8	11.1	11.1	11.1	11.1	10.7
9	3.7	3.7	3.7	3.7	4.1
10	1.4	1.4	1.4	1.4	1.6

Low Latitude (15°)

	Total Ozone (D.U.)		
Layer	225	275	325
0,1	24.0	24.0	24.0
2	5.0	6.0	10.0
3	7.0	16.0	31.0
4	25.0	52.0	71.0
5	62.2	75.2	87.2
6	57.0	57.0	57.0
7	29.4	29.4	29.4
8	10.9	10.9	10.9
9	3.2	3.2	3.2
10,11,12	1.3	1.3	1.3

APPENDIX E DATA AVAILABILITY

The derivative tape and CD-ROM products defined in this User's Guide are archived and available from the National Space Science Data Center (NSSDC). The NSSDC may establish a nominal charge for production and dissemination of data requested.

Domestic requests for data should be addressed to the following address:

National Space Science Data Center
NASA/Goddard Space Flight Center
Code 633.4
Greenbelt, MD 20771
Telephone: (301) 286-6695
FAX number: (301) 286-1771

All requests from foreign researchers must be specifically addressed to

Director, World Data Center A for Rockets
and Satellites
NASA/Goddard Space Flight Center
Code 633.4
Greenbelt, MD 20771 USA
Telephone: (301) 286-6695
FAX Number: (301) 286-1771

When ordering data from either NSSDC or the World Data Center, a user should specify why the data are needed, the subject of the work, the name of the organization with which the user is connected, and any Government contracts under which the study is being performed. Each request should specify the experiment data desired, the time period of interest, and any other information that would facilitate the handling of the data request.

A user requesting data on magnetic tapes should provide additional information concerning the plans for using the data, i.e., what computers and operating systems will be used. In this context, the NSSDC is compiling a library of routines that can unpack or transform the contents of many of the data sets into formats that are appropriate for the user's computers. NSSDC will provide, upon request, information concerning its services. When requesting data on magnetic tape, the user must specify whether he or she will supply new tapes prior to the processing, or return the original NSSDC tapes after the data have been copied.

Data product order forms may be obtained from NSSDC/World Data Center A. Some data requests and actual data acquisition can be accomplished using an interactive dial-in capability for PC and modem. For information about this system or data availability in general, call the NSSDC Request Hot-line at (301) 286-6695. Also, electronic mail can be directed to NSSDC::REQUEST through NSI/DECNET or REQUEST@NSSDCA.GSFC.NASA.GOV through INTERNET.

REPORT DOCUMENTATION PAGE

Form Approved
OMB No. 0704-0188

1. AGENCY USE ONLY *(Leave blank)*	2. REPORT DATE	3. REPORT TYPE AND DATES COVERED
	November 1993	Reference Publication

4. TITLE AND SUBTITLE

Nimbus–7 Total Ozone Mapping Spectrometer (TOMS) Data Products User's Guide

5. FUNDING NUMBERS

Code 916
NAS 5–29386

6. AUTHOR(S)

Richard D. McPeters, Arlin J. Krueger, P.K. Bhartia, Jay R. Herman, Arnold Oaks, Ziuddin Ahmad, Richard P. Cebula, Barry M. Schlesinger, Tom Swissler, Steven L. Taylor, Omar Torres, and Charles G. Wellemeyer

7. PERFORMING ORGANIZATION NAME(S) AND ADDRESS(ES)

Goddard Space Flight Center
Greenbelt, Maryland 20771

8. PERFORMING ORGANIZATION REPORT NUMBER

94B00013

9. SPONSORING/MONITORING AGENCY NAME(S) AND ADDRESS(ES)

National Aeronautics and Space Administration
Washington, D.C. 20546–0001

10. SPONSORING/MONITORING AGENCY REPORT NUMBER

NASA RP–1323

11. SUPPLEMENTARY NOTES

Authors Ahmad, Cebula, Schlesinger, Swissler, Taylor, Torres, and Wellemeyer: Hughes STX Corporation (HSTX), 4400 Forbes Boulevard, Lanham, Maryland, 20706.

12a. DISTRIBUTION/AVAILABILITY STATEMENT

Unclassified–Unlimited
Subject Category 47
Report available from the NASA Center for AeroSpace Information, 800 Elkridge Landing Road, Linthicum Heights, MD 21090; (301) 621–0390.

12b. DISTRIBUTION CODE

13. ABSTRACT *(Maximum 200 words)*

Two tape products from the Total Ozone Mapping Spectrometer (TOMS) aboard the Nimbus–7 have been archived at the National Space Science Data Center. The instrument measures backscattered Earth radiance and incoming solar irradiance; their ratio—the albedo—is used in ozone retrievals. In–flight measurements are used to monitor changes in the instrument sensitivity. The algorithm to retrieve total column ozone compares the observed ratios of albedos at pairs of wavelengths with pair ratios calculated for different ozone values, solar zenith angles, and optical paths. The initial error in the absolute scale for TOMS total ozone is 3 percent, the one standard–deviation random error is 2 persent, and the drift is $\pm$ 1.5 percent over 14.5 years. The High Censity TOMS (HDTOMS) tape contains the measured albedos, the derived total ozone amount, reflectivity, and cloud–height information for each scan position. It also contains an index of SO_2 contamination for each position. The Gridded TOMS (GRIDTOMS) tape contains daily total ozone and reflectivity in roughly equal area grids (110 km in latitude by about 100–150 km in longitude). Detailed descriptions of the tape structure and record formats are provided.

14. SUBJECT TERMS

Total Ozone Mapping Spectrometer, Ozone, Sulfur Dioxide, Reflectivity

15. NUMBER OF PAGES

89

16. PRICE CODE

17. SECURITY CLASSIFICATION OF REPORT	18. SECURITY CLASSIFICATION OF THIS PAGE	19. SECURITY CLASSIFICATION OF ABSTRACT	20. LIMITATION OF ABSTRACT
Unclassified	Unclassified	Unclassified	Unlimited